

SUPPORTING INFORMATION

# **Porous Dipeptide Crystals as Volatile-Drug Vessels**

*Silvia Bracco, Donata Asnaghi, Mattia Negroni, Piero Sozzani  
and Angiolina Comotti\**

Department of Material Science,  
University of Milano-Bicocca and INSTM Consortium  
Via Roberto Cozzi 55, 20125 Milano, Italy

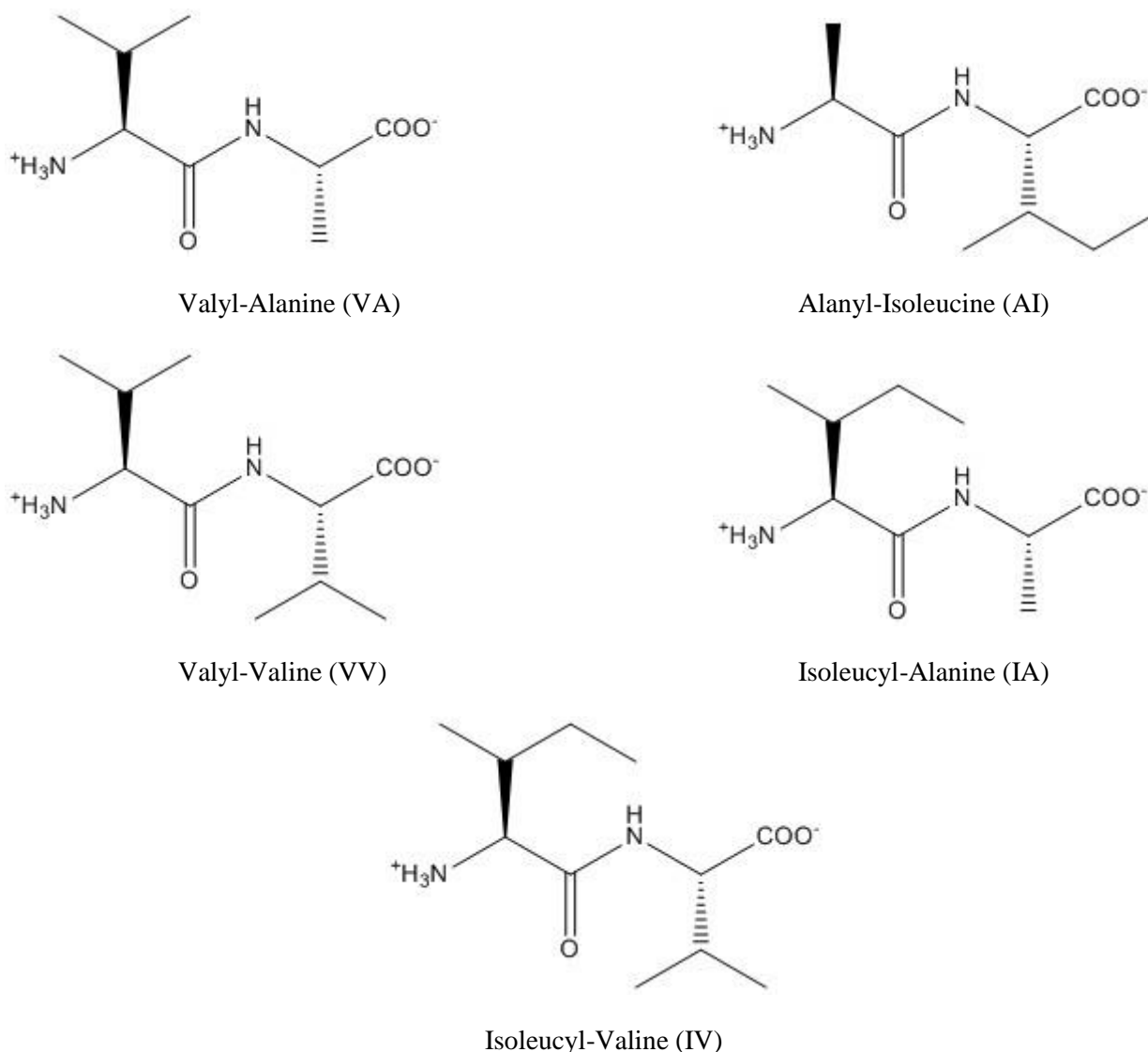
## Table of Contents

<b>1. General methods</b>	<b>p. S3</b>
<b>1.1 Sample preparation</b>	<b>p. S3</b>
<b>1.2 Volumetric adsorption measurements</b>	<b>p. S3</b>
<b>1.3 Powder X-ray diffraction analyses</b>	<b>p. S4</b>
<b>1.4 Ab initio calculations</b>	<b>p. S4</b>
<b>1.5 Solution NMR experiments</b>	<b>p. S4</b>
<b>1.6 Solid state NMR experiments</b>	<b>p. S4</b>
<b>1.7 Dynamic Light Scattering experiments</b>	<b>p. S5</b>
<b>2. Crystallographic and physico-chemical data</b>	<b>p. S6</b>
<b>3. Crystal structures</b>	<b>p. S6</b>
<b>4. Powder diffraction patterns</b>	<b>p. S8</b>
<b>5. Isothermic heats of adsorption</b>	<b>p. S9</b>
<b>6. Adsorption isotherms</b>	<b>p. S10</b>
<b>7. Conformational analysis and simulated NMR</b>	<b>p. S16</b>
<b>8. <math>^{19}\text{F}</math> and <math>^{13}\text{C}</math> Solution NMR spectra</b>	<b>p. S17</b>
<b>9. <math>^{19}\text{F}</math>, <math>^{13}\text{C}</math> and <math>^1\text{H}</math> Solid State NMR spectra</b>	<b>p. S21</b>
<b>10. Kinetics of adsorption experiments</b>	<b>p. S35</b>
<b>11. Adsorption and desorption curves</b>	<b>p. S38</b>
<b>12. GCMC simulation of isotherms</b>	<b>p. S42</b>
<b>13. Dynamic Light Scattering results</b>	<b>p. S45</b>
<b>14. References</b>	<b>p. S45</b>

## 1. General methods

### 1.1 Sample preparation

L-valyl-L-alanine (Val-Ala), L-alanyl-L-isoleucine (Ala-Ile), L-valyl-L-valine (Val-Val), L-isoleucine-L-alanine (Ile-Ala) and ), L-isoleucyl-L-valine (Ile-Val) were purchased from Bachem company. The samples underwent thermal treatment at 60°C in vacuum ( $10^{-3}$  torr) for 8 hours and at room temperature for 12 hours. Diethylether and halothane were purchased from Sigma-Aldrich, while enflurane from Alfa Aesar and isoflurane from TCI Chemicals. Before the adsorption measurements the vapors have been purified by gaseous residues with a freeze and thaw process.



**Scheme 1.** Dipeptide chemical structures.

### 1.2 Volumetric adsorption measurements

The dipeptide crystalline powders were treated under vacuum at 60° C for 10 hours and room temperature for 12 hours. Adsorption isotherms of halogenated and diethyl ethers were performed by volumetric measurements using a home-made apparatus equipped with 3 pressure gauge. The

measurements were carried out at 273 K and at 298 K. The maximum pressure values used for the adsorption measurements were set according to the anesthetic vapor pressures. The adsorption kinetics data were collected for 20 minutes and adsorption equilibrium values were reported in the isotherms. The isosteric heats of adsorption were calculated at low surface coverage applying the Clausius-Clapeyron equation.

### 1.3 Powder X-ray diffraction

The dipeptide crystalline powders were treated under vacuum at 60° C for 10 hours and room temperature for 12 hours. The samples were transferred into capillaries (1 mm diameter) under inert atmosphere and evacuated at room temperature for a few hours ( $10^{-3}$  torr), then they were loaded with halogenated molecules by sorption from the gas phase at 298 K and the capillaries were sealed. Powder X-ray diffraction measurements were carried out using a Panalytical X'Pert PRO with PIXcel detector and incident-beam focusing mirror. The radiation wavelength  $\lambda$  was Cu  $K_{\alpha}$  (1.54056 Å). The  $2\theta$  range between 4° and 80°, with steps of 0.013° (360 s for each step), was investigated. The interplanar distances were indexed considering the hexagonal crystal system ( $P6_1$  space group). The refined unit cell parameters are reported in Table S2.

### 1.4 Ab initio calculations

The computational study was performed using the Gaussian03 software. The dihedral angles  $\theta_1$  (C-C-O-C) and  $\theta_2$  (C-O-C-H) for isoflurane and  $\theta_1$  (Cl-C-C-O),  $\theta_2$  (C-C-O-C) and  $\theta_3$  (C-O-C-H) for enflurane were explored by incremental steps of 15° in order to localize the most stable conformers. For isoflurane, the structural optimizations and the frequency calculations were performed with the B3LYP/6-311G++(2df,p) hybrid density functional method. For enflurane, the structural optimization was performed with the B3LYP/6-311G++(2d,2p) hybrid density functional method, whereas the frequency calculation with the B3LYP/6-31G (2d) DFT method. The NMR chemical shifts and J couplings were calculated applying the B3LYP/6-311G++(2df,p) GIAO method for both the molecules.

### 1.5 Solution NMR experiments

$^{13}\text{C}$  NMR spectra,  $^{19}\text{F}$  NMR and  $^{19}\text{F}$  decoupled from  $^1\text{H}$  NMR spectra of the samples in  $\text{CDCl}_3$  were recorded on a Bruker AVANCE NEO 400 MHz, SmartProbe™ equipped with 2 channels and  $^2\text{H}$  lock channel.

### 1.6 Solid State NMR experiments

Solid-state  $^1\text{H}$  MAS NMR spectra (single-pulse experiment SPE) were performed with a Bruker Avance III 600 MHz instrument operating at 14.1 T, using a recycle delay of 20 s. A MAS Bruker probe head was used with 2.5 mm  $\text{ZrO}_2$  rotors spinning at 30 kHz. The 90° pulse for proton was 2.9  $\mu\text{s}$ . The  $^1\text{H}$  chemical shift was referenced to adamantane. Spectral profiles were fit by Lorentzian line shapes.

Solid-state NMR spectra were run at 75.5 MHz for  $^{13}\text{C}$  and at 282.4 MHz for  $^{19}\text{F}$  MHz on a Bruker Avance 300 instrument operating at a static field of 7.04 T equipped with high-power amplifiers (1 kW) and a 4 mm double resonance MAS probe.  $^{13}\text{C}\{^1\text{H}\}$  ramped-amplitude cross polarization (CP) experiments were performed at a spinning speed of 8 kHz and 12.5 kHz, using a contact time of 5

ms. The 90° pulse used for proton was 2.9 μs. <sup>13</sup>C {<sup>1</sup>H} single-pulse excitation (SPE) experiments were run using a recycle delay of 10 s and a 90° pulse of 4.5 μs. <sup>13</sup>C{<sup>19</sup>F} ramped-amplitude cross polarization (CP) experiments were performed at a spinning speed of 8 kHz, using a 90° pulse of 3.2 μs and a contact time of 5 ms. <sup>13</sup>C {<sup>19</sup>F} SPE experiments were run using a recycle delay of 30 s, a 90° pulse of 3.65 μs and a spinning speed of 5 kHz. Crystalline polyethylene was taken as an external reference at 32.8 ppm from TMS. <sup>19</sup>F SPE MAS NMR spectra were collected using a 90° pulse of 3.2 μs and a recycle delay of 20 s. The <sup>19</sup>F chemical shift was referenced to NaF. The spectra were collected at 249 K and 300 K.

The dipeptide crystalline powders were treated under vacuum at 60° C for 10 hours and room temperature for 12 hours, then they were transferred into the NMR rotors (4 mm for <sup>13</sup>C and <sup>19</sup>F NMR and 2.5 mm for <sup>1</sup>H NMR) under dry N<sub>2</sub> atmosphere and evacuated at room temperature for a few hours (10<sup>-3</sup> torr). They were loaded with halogenated molecules by following the adsorption isotherms at 273-298 K, when the maximum adsorption was reached the rotors were sealed.

### 1.7 Gran Canonical Monte Carlo simulations

Grand Canonical Monte Carlo simulations were applied to calculate the adsorption isotherms of the porous VA. The geometry optimized structures of enflurane and isoflurane were used. The CVFF and Universal force fields for enflurane and isoflurane were applied. The Lennard-Jones cut-off distance was set to 14 Å. The simulation box consists of a supercell of 2 × 2 × 3 crystallographic units with fixed atom positions of VA. All simulations include 8 × 10<sup>6</sup> cycle equilibration periods. The temperature was set at 298K. The Ewald sum technique was used to compute the electrostatic interactions

### 1.8 Dynamic Light Scattering experiments

Malver Zetasizer equipped with a continuous wave 1 mW He-Ne laser operating at 632.6 nm and an avalanche photodiode detector placed at 173° with respect to the incident beam was used. The sample was dispersed in toluene (concentration of 2 mg/ml) and sonicated for 1 h.

## 2. Crystallographic and physico-chemical data

**Table S1.** Physico-chemical properties of halogenated and diethyl ethers.

Molecule	Molecular weight (g/mol)	Vapor tension (kPa at 20°C)	Density (g/mL)	Boiling point (°C)	Volume (Å <sup>3</sup> )
Diethyl ether	74.12	58.66	0.71	34.6	85.4
Halothane (2-bromo-2-chloro-1,1,1-trifluoroethane)	197.4	32	1.86	50.2	88.7
Enflurane (2-chloro-1,1,2-trifluoroethyl-difluoromethyl ether)	184.5	23	1.51	56.5	110.3
Isoflurane (2-chloro-2,2,2-trifluoroethyl-difluoromethyl ether)	184.5	32	1.51	48.5	108.3
Desflurane (1,2,2,2-tetrafluoroethyl difluoromethyl ether)	168	88.5	1.46	23.5	134.8

## 3. Crystal Structures

**Dipeptide Crystals.** The dipeptide crystals of VA, AI, VV, IA and IV form a hexagonal unit cell (space group P6<sub>1</sub>). The pore volume was estimated by considering a sphere of 2 Å of the crystal channels and a grid of 0.5 Å (contact surface) (Mercury CSD 3.9). The pore diameter was estimated by a cylindrical model  $r = (V_{\text{empty}} / \pi c)^{1/2}$ .<sup>[1-4]</sup> The van der Waals radii were considered for the measurement of the pore size. The Connolly surface was described by a radius of 1.3 Å, an interval of 0.15 Å and ultra-fine grid resolution.

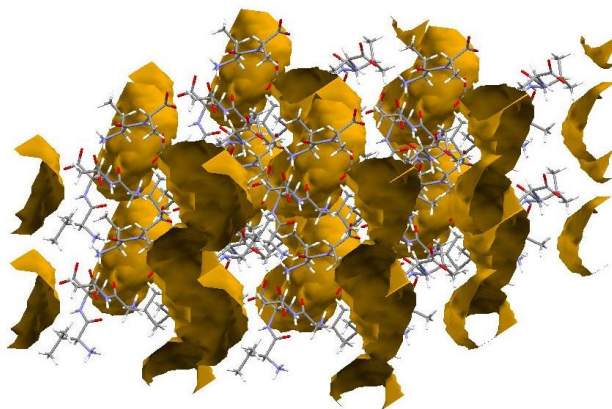
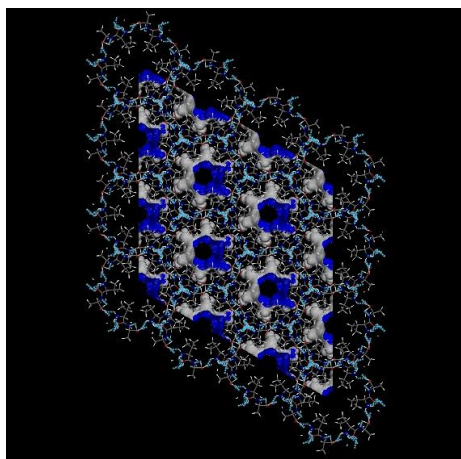


**Figure S1.** Valyl-Alanine VA channels (*c*-axis view): Connolly surface (blue/grey) and hydrogen bonds (light-blue) (left). Crystal channels of VA dipeptide: cross-section of 5.1-5.3 Å (left).

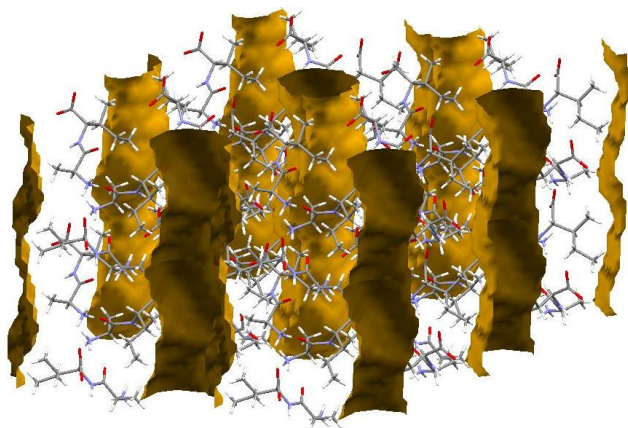
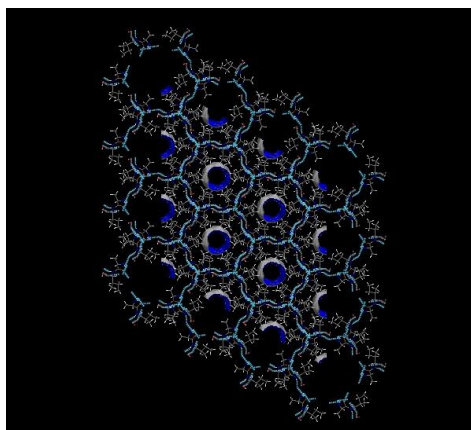


**Figure S2.** Alanyl-Isoleucine (AI) channels (*c*-axis view): Connolly surface (blue/grey) and hydrogen bonds (light-blue) (left). Crystal channels of AI dipeptide: cross-section of 4.7-5.0 Å (right).

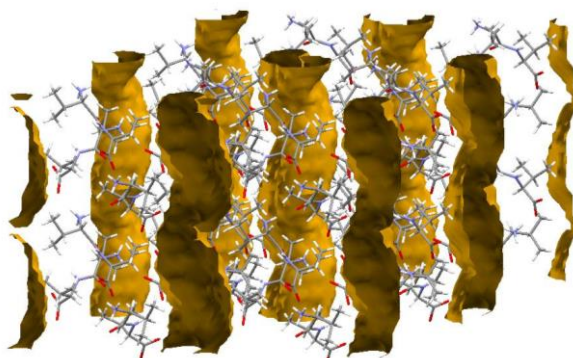
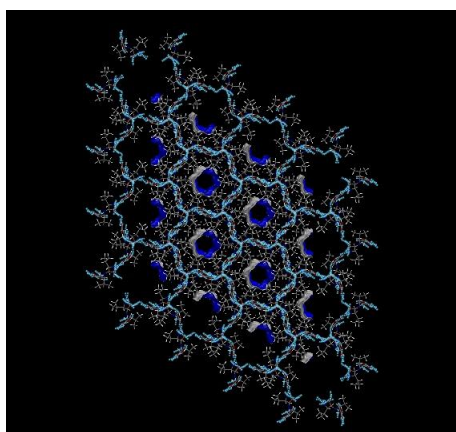


**Figure S3.** Valyl-Valine (VV) channels (*c*-axis view): Connolly surface (blue/grey) and hydrogen bonds (light-blue) (left). Crystal channels of VV dipeptide: cross-section of 4.0-4.2 Å (left).

#### 4. Powder diffraction patterns

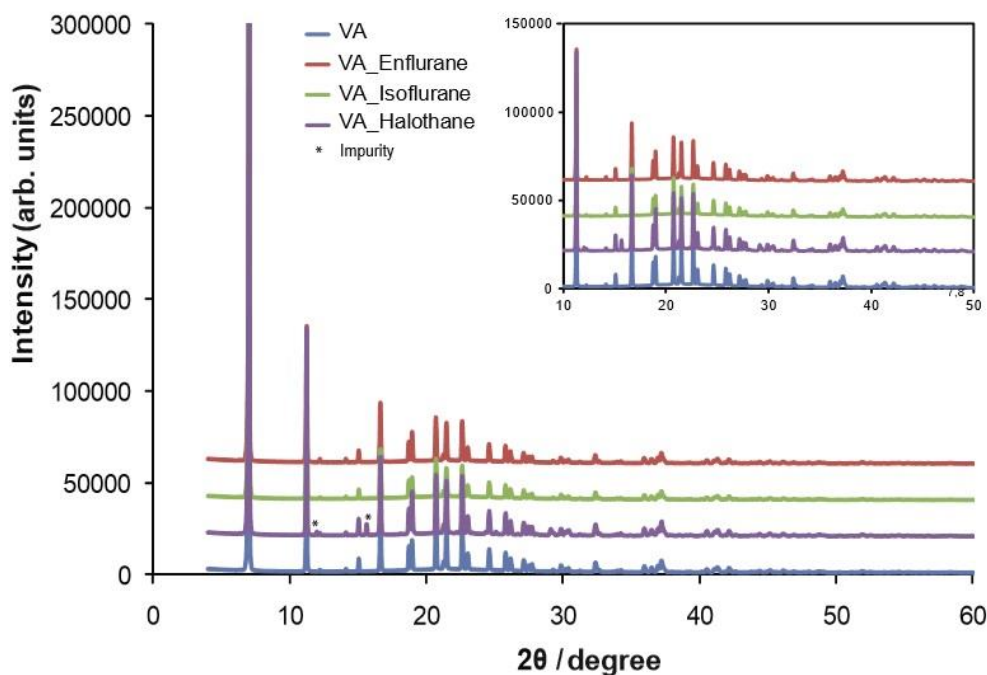


**Figure S4.** Powder X-ray diffraction patterns of empty Valyl-Alanine (blue) and with halogenated guests (red, enflurane; green, isoflurane; purple, halothane). The unit cell parameters of empty VA are the following:  $a=14.46 \text{ \AA}$ ,  $c=10.08 \text{ \AA}$ ,  $V=1826.03 \text{ \AA}^3$ ,  $\sigma=1 \times 10^{-4}$ .

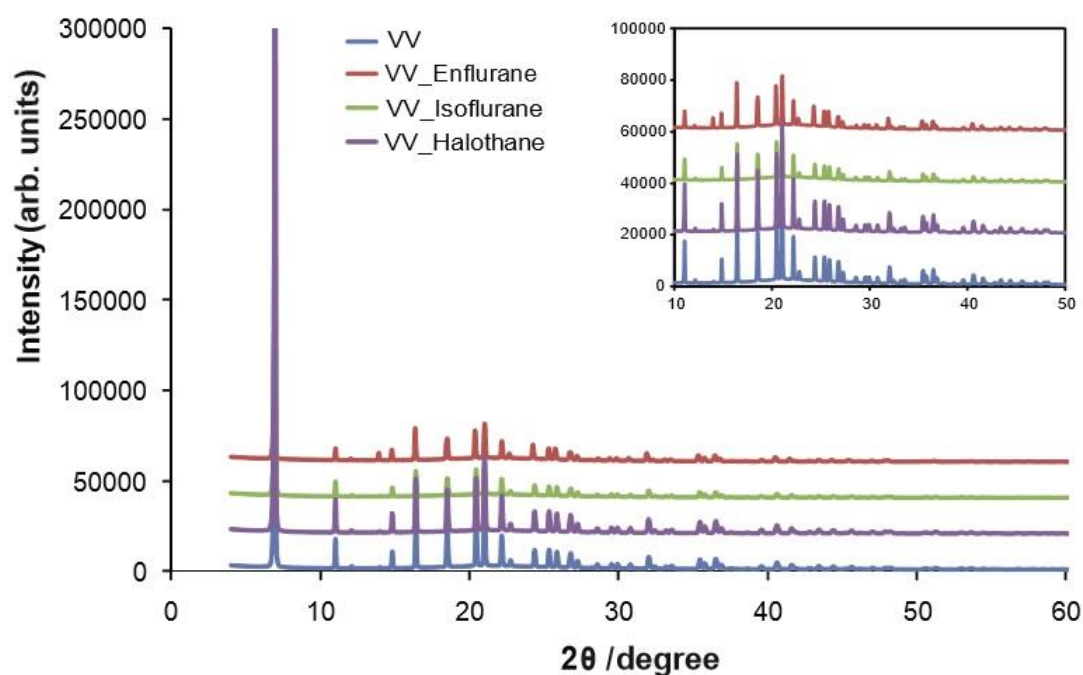


**Figure S5.** Powder X-ray diffraction patterns of empty Valyl-Valine (blue) and with the guests (red, enflurane; green, isoflurane; purple, halothane). The unit cell parameters of the empty VV are the

following:  $a=14.64 \text{ \AA}$ ,  $c=10.34 \text{ \AA}$ ,  $V=1918.38 \text{ \AA}^3$ ,  $\sigma=6 \times 10^{-4}$ . The unit cell parameters of VV/enflurane are the following:  $a=14.66 \text{ \AA}$ ,  $c=10.35 \text{ \AA}$ ,  $V=1927.74 \text{ \AA}^3$ ,  $\sigma=8 \times 10^{-4}$ .

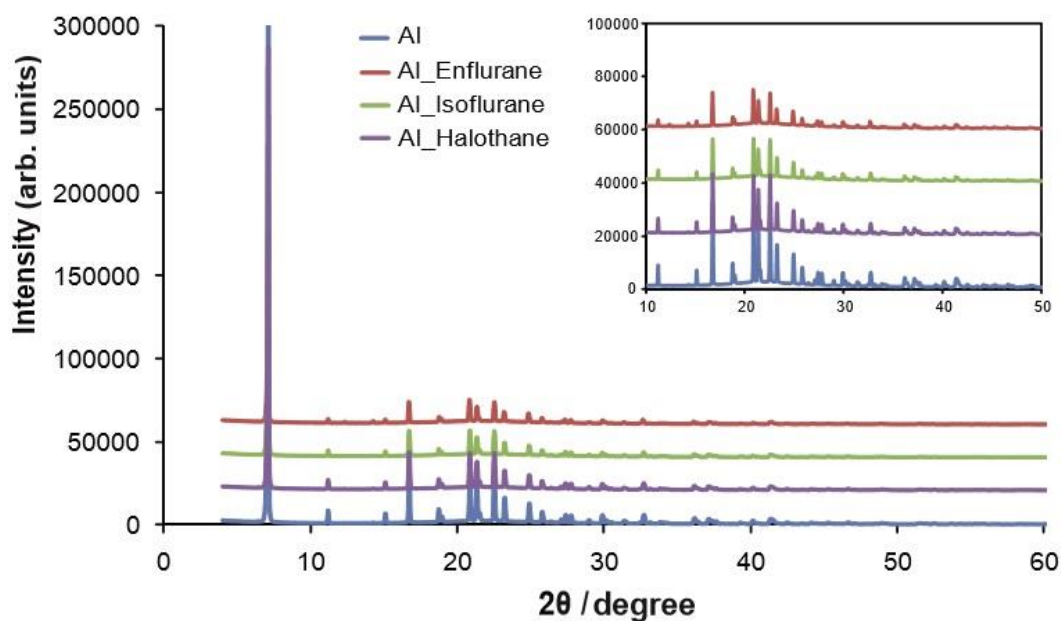


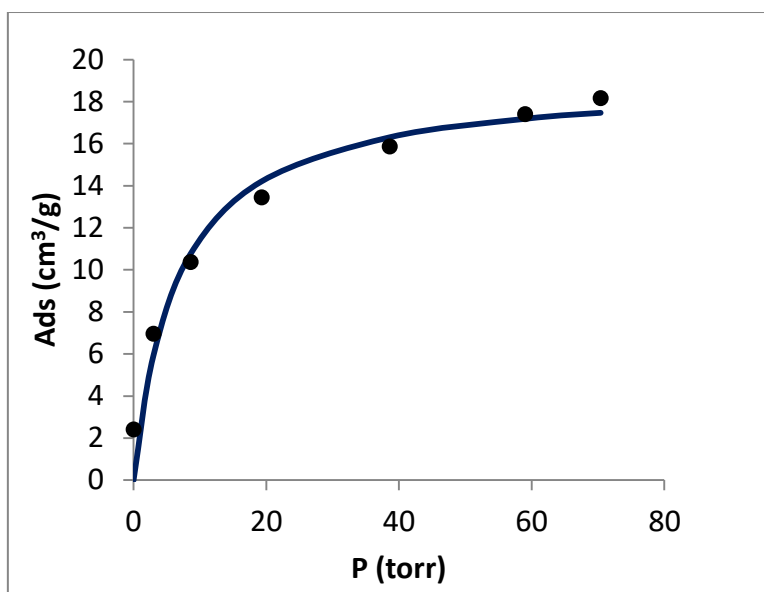
**Figure S6.** Powder X-ray diffraction patterns of empty Alanyl-Isoleucine (blue) and with the guests (red, enflurane; green, isoflurane; purple, halothane). The unit cell parameters of the empty AI are the following:  $a=14.12 \text{ \AA}$ ,  $c=10.02 \text{ \AA}$ ,  $V=1729.60 \text{ \AA}^3$ ,  $\sigma=2.6 \times 10^{-4}$ . The unit cell parameters of VV/enflurane are the following:  $a=14.17 \text{ \AA}$ ,  $c=10.18 \text{ \AA}$ ,  $V=1769.80 \text{ \AA}^3$ ,  $\sigma=2.0 \times 10^{-4}$ .

## 5. Isosteric heats of adsorption

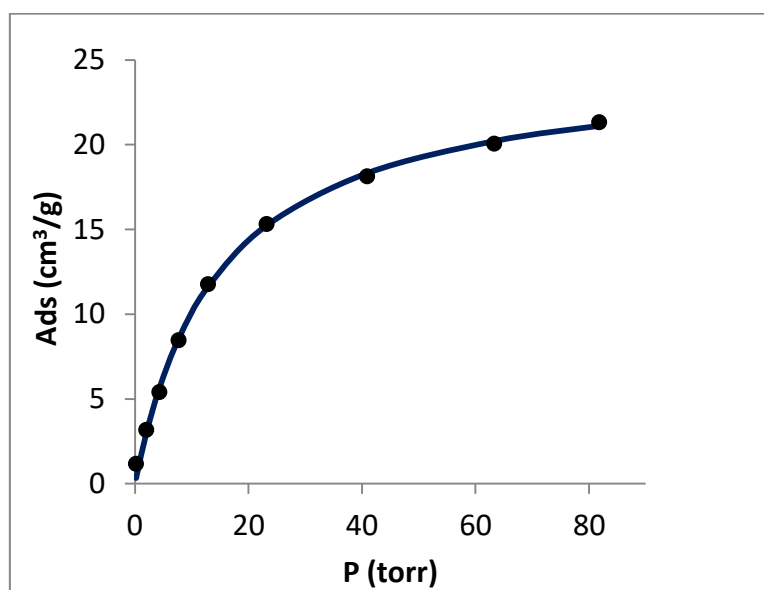
**Table S2.** Isosteric heats of adsorption of halogenated ethers in dipeptide crystals.

	$\Delta H$ (kJ/mol)
<b>Valyl-Alanine (VA)</b>	
Enflurane	54.70
Isoflurane	32.70
Halothane	42
<b>Alanyl-Isoleucine (AI)</b>	
Enflurane	n.d.
Isoflurane	37.70
Halothane	39.80
<b>Valyl-Valine (VV)</b>	
Enflurane	39.60
Isoflurane	37.60
Halothane	40.70

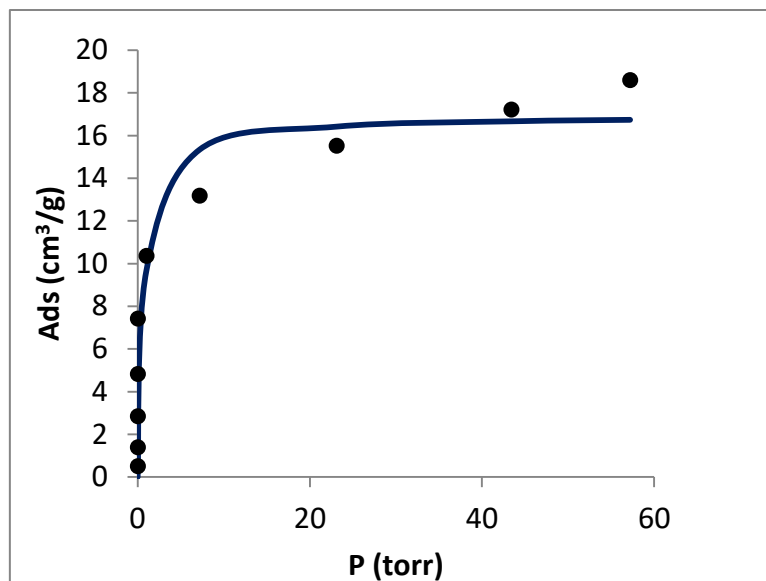
## 6. Adsorption isotherms



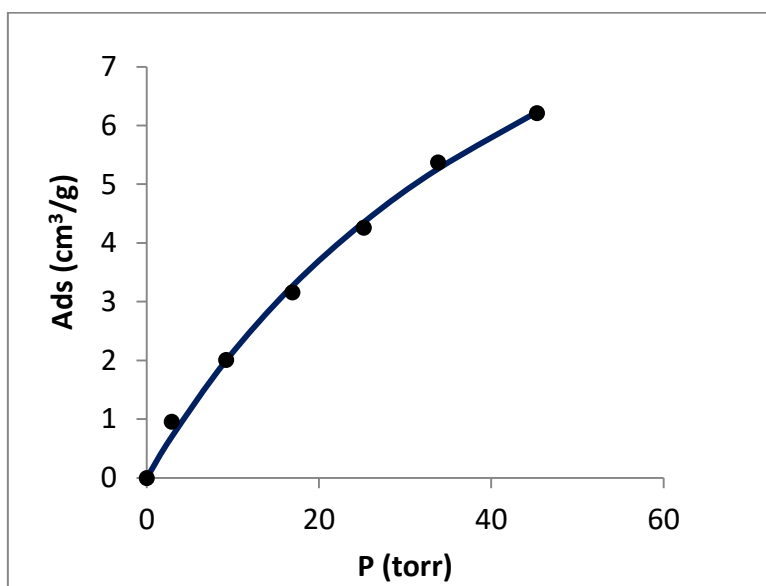
**Figure S7.** Adsorption isotherm of isoflurane in VA at 273K (non linear square fitting of Langmuir equation:  $M= 19 \text{ cm}^3/\text{g}$ ,  $k = 0.15$ ).



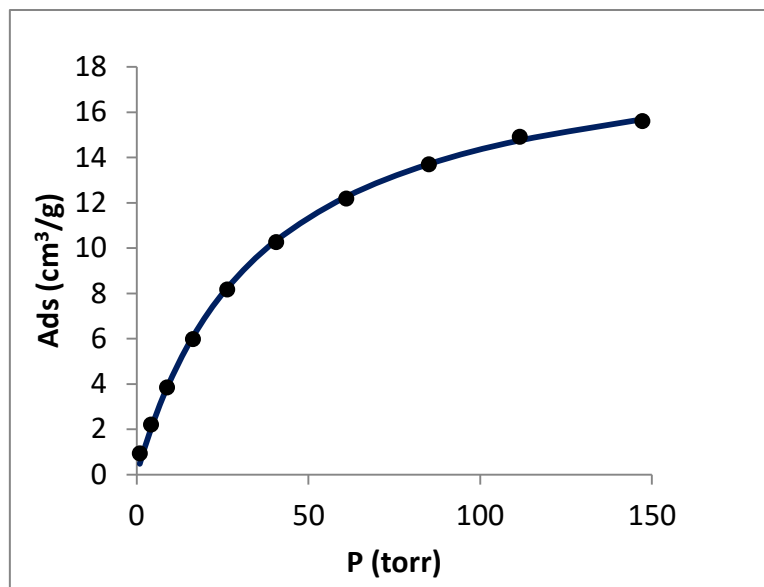
**Figure S8.** Adsorption isotherm of halothane in VA at 273K (non linear square fitting of Langmuir equation:  $M= 25 \text{ cm}^3/\text{g}$ ,  $k = 0.07$ ).



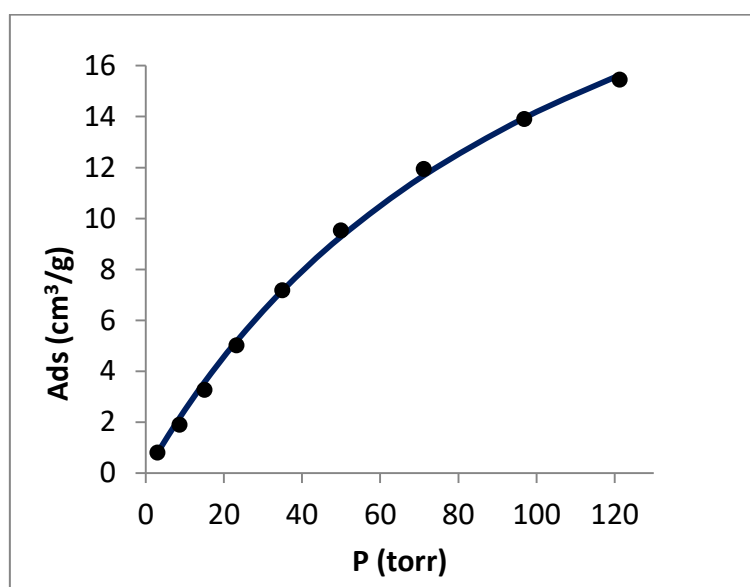
**Figure S9.** Adsorption isotherm of enflurane in VA at 273K (non linear square fitting of Langmuir equation:  $M=17 \text{ cm}^3/\text{g}$  and  $K=1.32 \text{ torr}^{-1}$ )



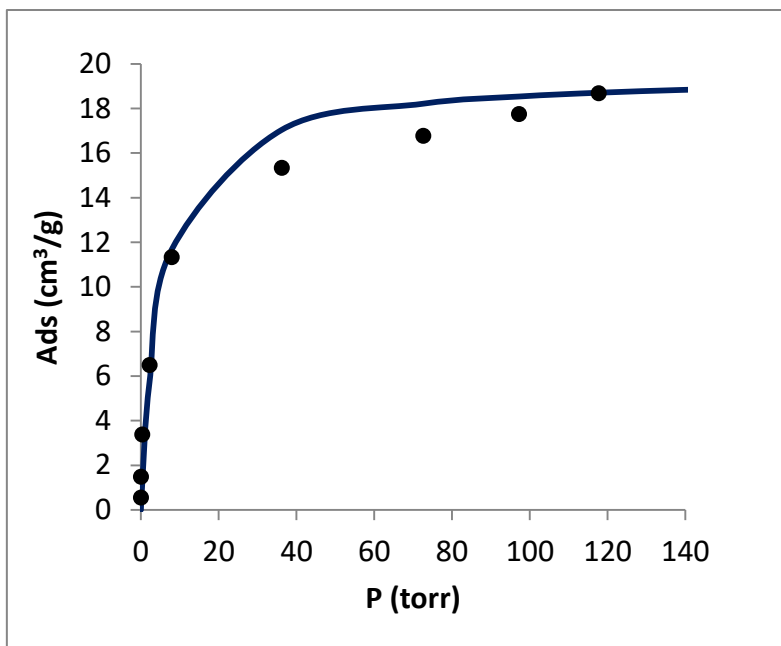
**Figure S10.** Adsorption isotherm of desflurane in VA at 273K (non linear square fitting of Langmuir equation:  $M=14 \text{ cm}^3/\text{g}$  and  $K=0.02 \text{ torr}^{-1}$ )



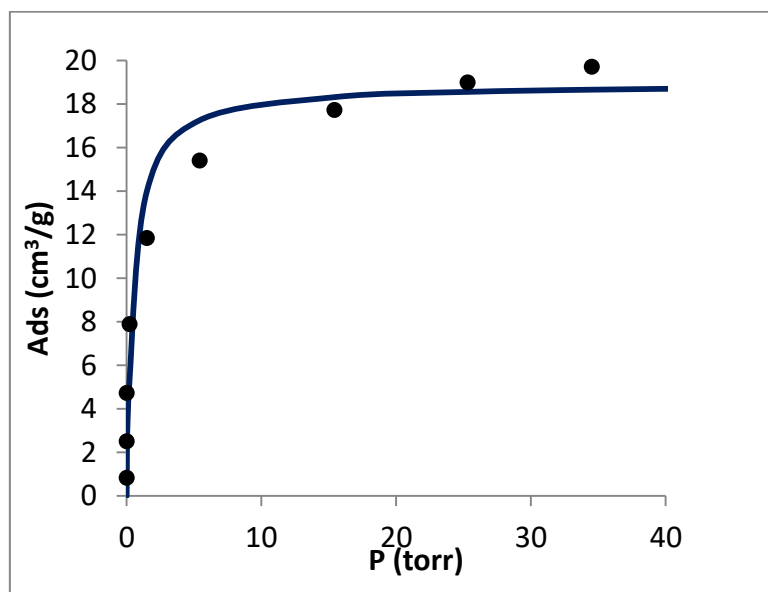
**Figure S11.** Adsorption isotherm of isoflurane in VA at 298K (non linear square fitting of Langmuir equation:  $M=19 \text{ cm}^3/\text{g}$  and  $K=0.03 \text{ torr}^{-1}$ )



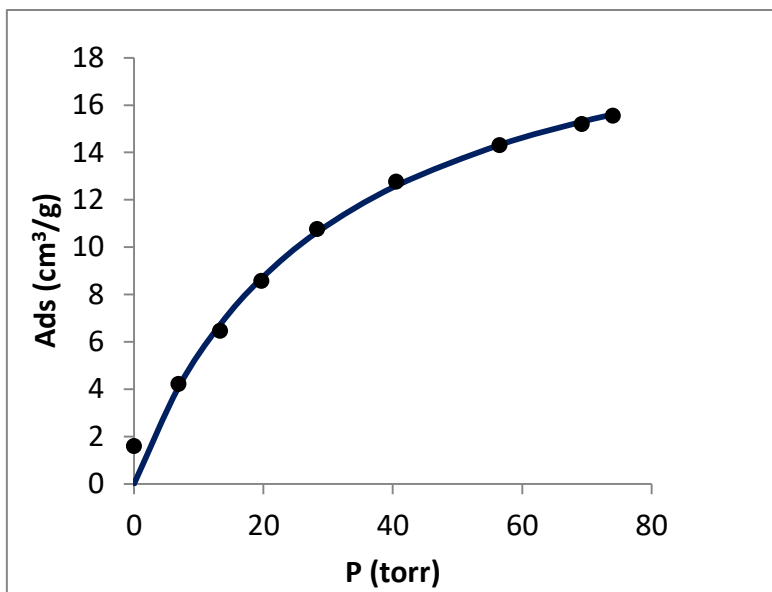
**Figure S12.** Adsorption isotherm of halothane in VA at 298K (non linear square fitting of Langmuir equation:  $M=30 \text{ cm}^3/\text{g}$  and  $K=0.01 \text{ torr}^{-1}$ )



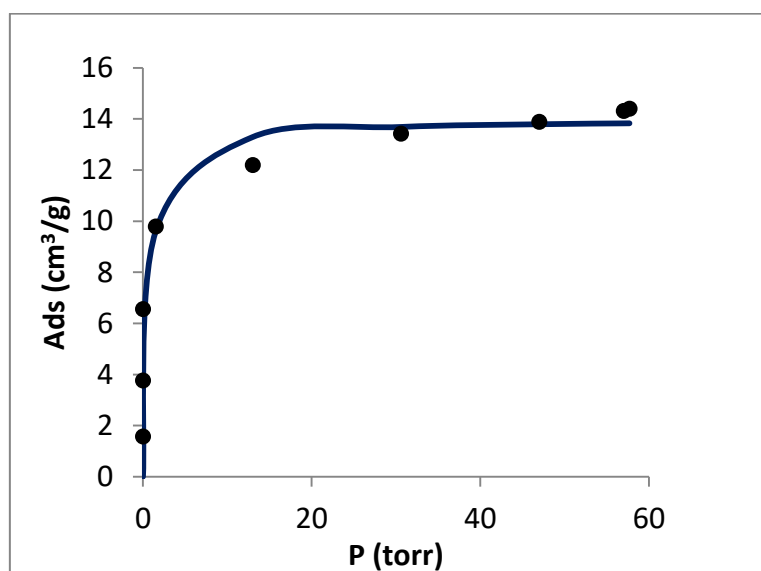
**Figure S13.** Adsorption isotherm of enflurane in VA at 298K (non linear square fitting of Langmuir equation:  $M=19 \text{ cm}^3/\text{g}$  and  $K=0.18 \text{ torr}^{-1}$ )



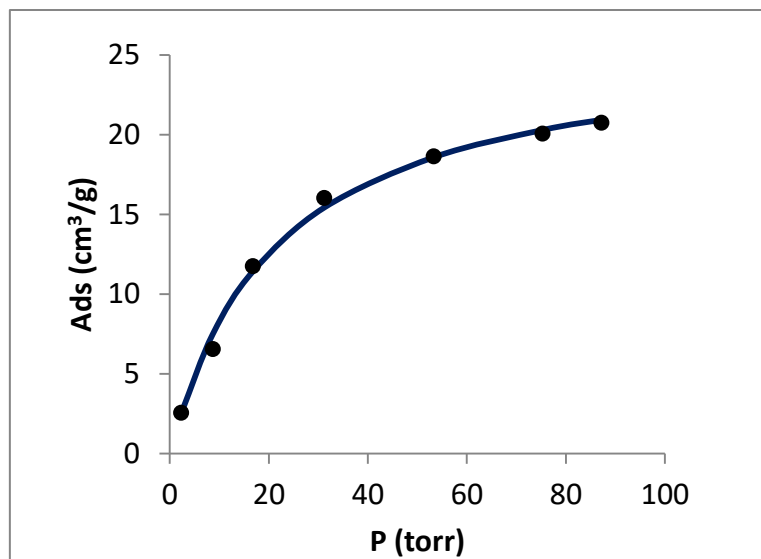
**Figure S14.** Adsorption isotherm of enflurane in VV at 273K (non linear square fitting of Langmuir equation:  $M=19 \text{ cm}^3/\text{g}$  and  $K=1.9 \text{ torr}^{-1}$ )



**Figure S15.** Adsorption isotherm of isoflurane in AI at 273K (non linear square fitting of Langmuir equation:  $M=22 \text{ cm}^3/\text{g}$  and  $K=0.03 \text{ torr}^{-1}$ )



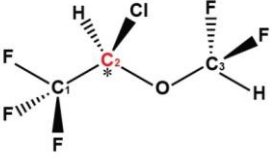
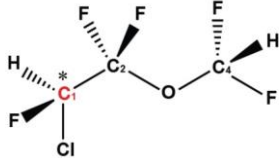
**Figure S16.** Adsorption isotherm of enflurane in AI at 273K (non linear square fitting of Langmuir equation:  $M=14 \text{ cm}^3/\text{g}$  and  $K=1.5 \text{ torr}^{-1}$ ).



**Figure S17.** Adsorption isotherm of halothane in AI at 273K (non linear square fitting of Langmuir equation:  $M=26 \text{ cm}^3/\text{g}$  and  $K=0.05 \text{ torr}^{-1}$ ).

## 7. Conformational analysis

Table S3. Conformers of isoflurane and enflurane.

Molecules	Minima	$\Delta E$ (Kcal/mol)
 <p data-bbox="328 595 459 629"><i>Isoflurane</i></p> <p data-bbox="288 663 496 696"><u>Dihedral angles</u></p> <p data-bbox="288 730 496 763"><math>\theta_1 = \text{C}_1\text{-C}_2\text{-O-C}_3</math></p> <p data-bbox="288 763 496 797"><math>\theta_2 = \text{C}_2\text{-O-C}_3\text{-H}</math></p>	Minimum 1 $\theta_1 = 139^\circ$ $\theta_2 = 179^\circ$	0
	Minimum 2 $\theta_1 = 166^\circ$ $\theta_2 = 59^\circ$	0.46
 <p data-bbox="328 1402 459 1435"><i>Enflurane</i></p> <p data-bbox="288 1469 496 1503"><u>Dihedral angles</u></p> <p data-bbox="288 1536 496 1570"><math>\theta_1 = \text{Cl-C}_1\text{-C}_2\text{-F}</math></p> <p data-bbox="288 1570 496 1603"><math>\theta_2 = \text{C}_1\text{-C}_2\text{-O-C}_4</math></p> <p data-bbox="288 1603 496 1637"><math>\theta_3 = \text{C}_2\text{-O-C}_4\text{-H}</math></p>	Minimum 1 $\theta_1 = 63^\circ$ $\theta_2 = 177^\circ$ $\theta_3 = 11^\circ$	0
	Minimum 2 $\theta_1 = 63^\circ$ $\theta_2 = 177^\circ$ $\theta_3 = 19^\circ$	0.006
	Minimum 3 $\theta_1 = 178^\circ$ $\theta_2 = -178^\circ$ $\theta_3 = -15^\circ$	0.1
	Minimum 4 $\theta_1 = -60^\circ$ $\theta_2 = 179^\circ$ $\theta_3 = 16^\circ$	0.12
	Minimum 5 $\theta_1 = 63^\circ$ $\theta_2 = -59^\circ$ $\theta_3 = -111^\circ$	0.42
	Minimum 6 $\theta_1 = 178^\circ$ $\theta_2 = -57^\circ$ $\theta_3 = 146^\circ$	0.43
	Minimum 7 $\theta_1 = 178^\circ$ $\theta_2 = -59^\circ$ $\theta_3 = 136^\circ$	0.49

## 8. $^{19}\text{F}$ and $^{13}\text{C}$ Solution NMR spectra

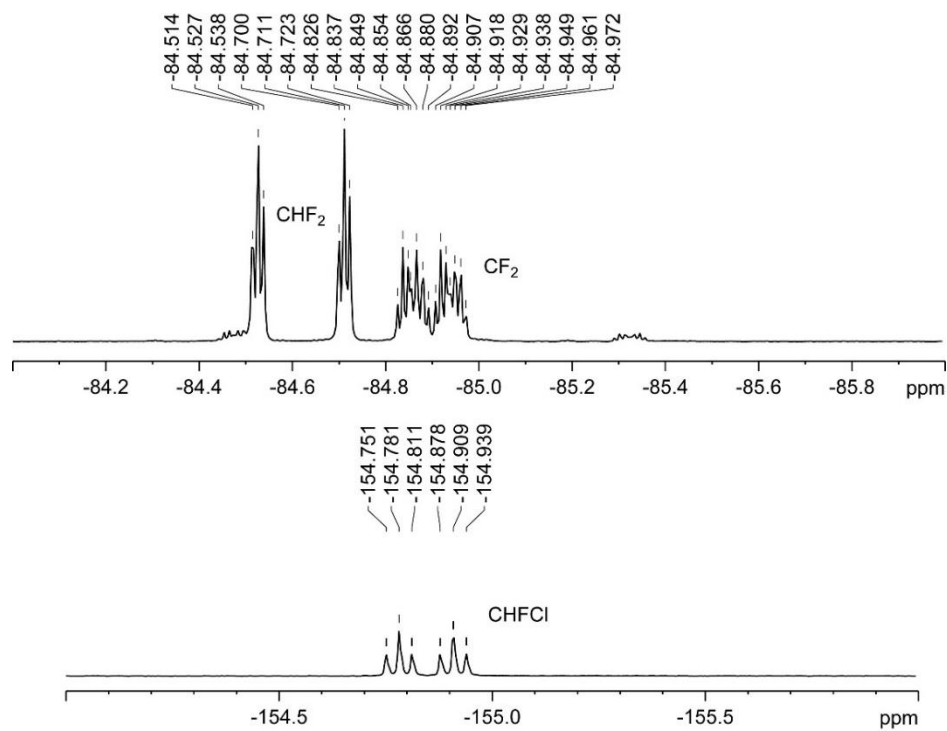


**Figure S18.**  $^{19}\text{F}$  NMR spectrum of enflurane in  $\text{CDCl}_3$ .

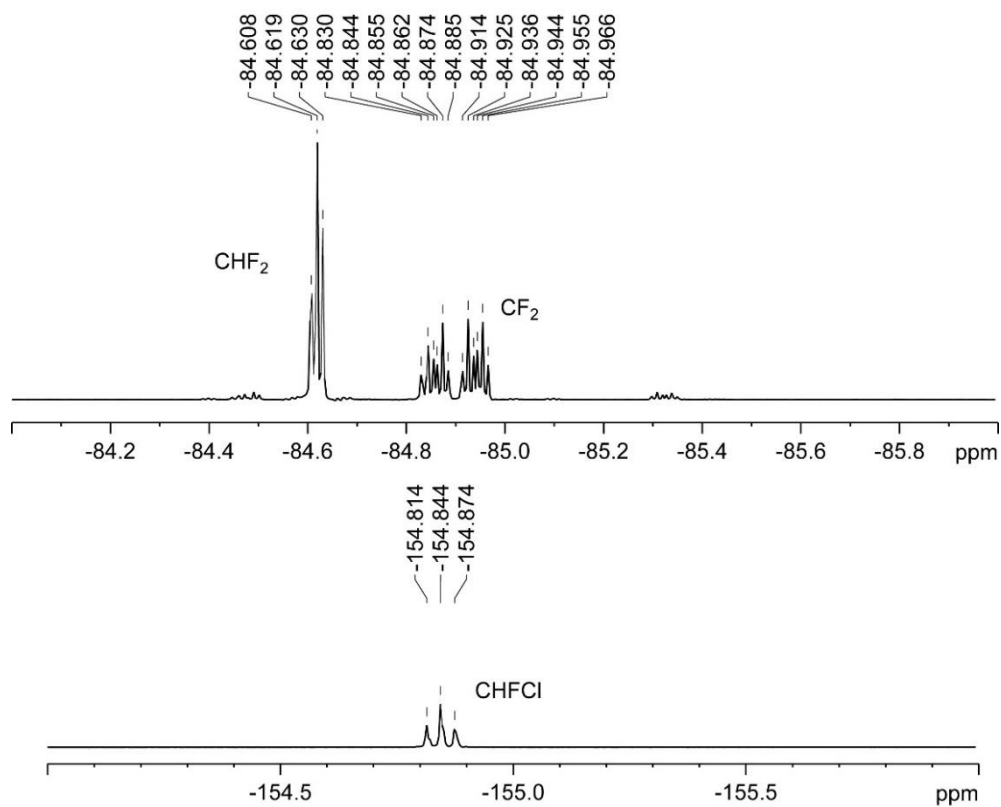


**Figure S19.**  $^{19}\text{F}$  (decouple from  $^1\text{H}$ ) NMR spectrum of enflurane in  $\text{CDCl}_3$ .

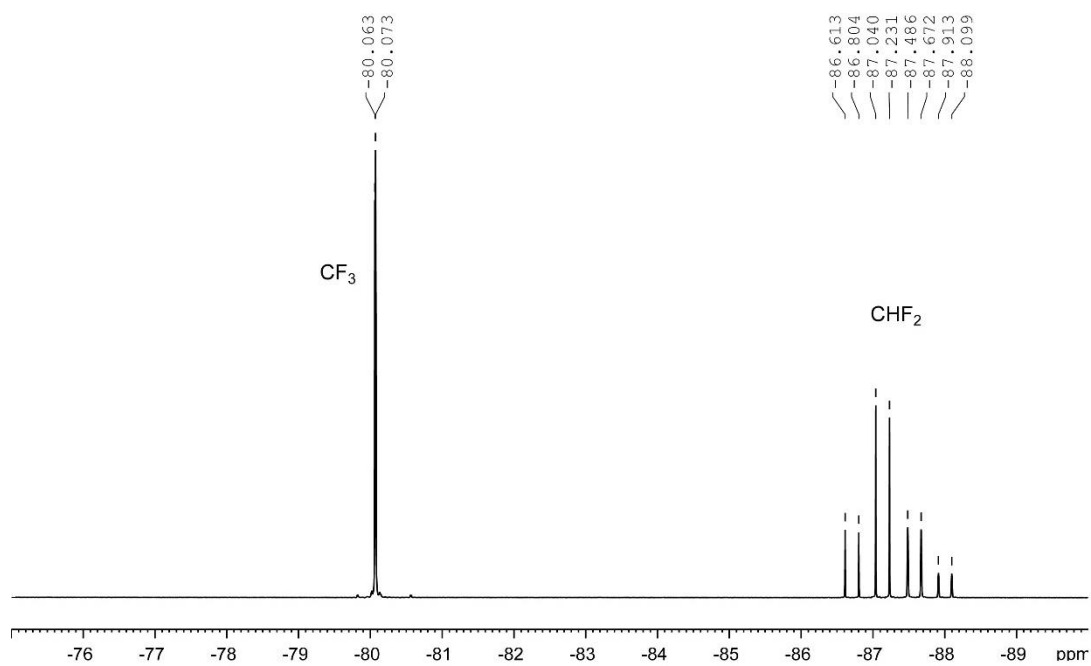


**Figure S20.** <sup>19</sup>F NMR spectrum of isoflurane in CDCl<sub>3</sub>.

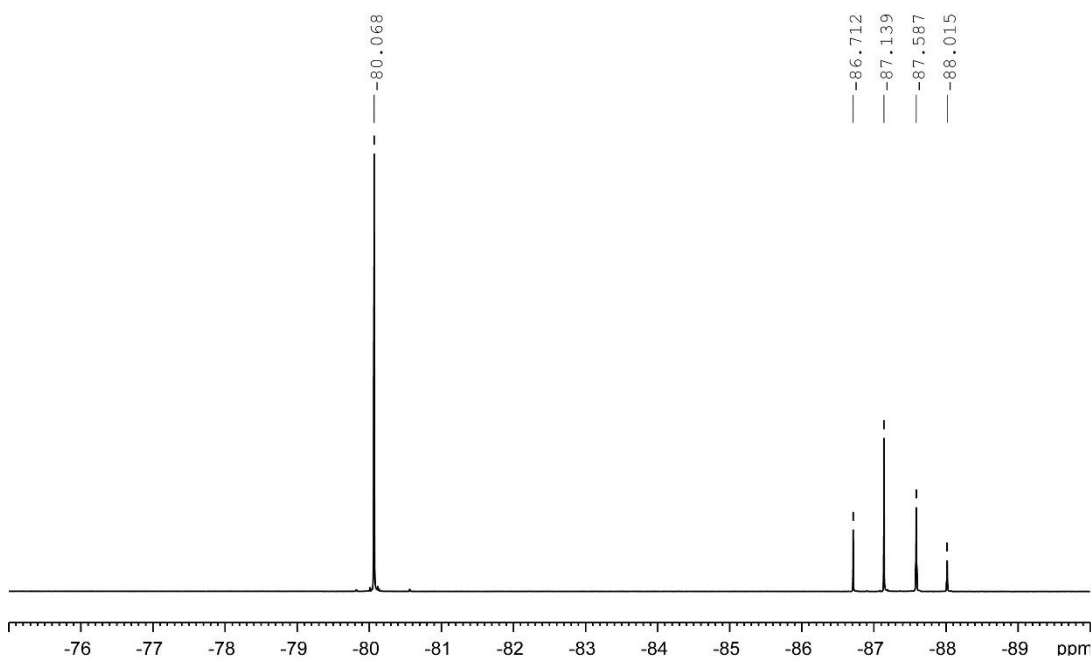


**Figure S21.** <sup>19</sup>F (decouple from <sup>1</sup>H) NMR spectrum of isoflurane in CDCl<sub>3</sub>.

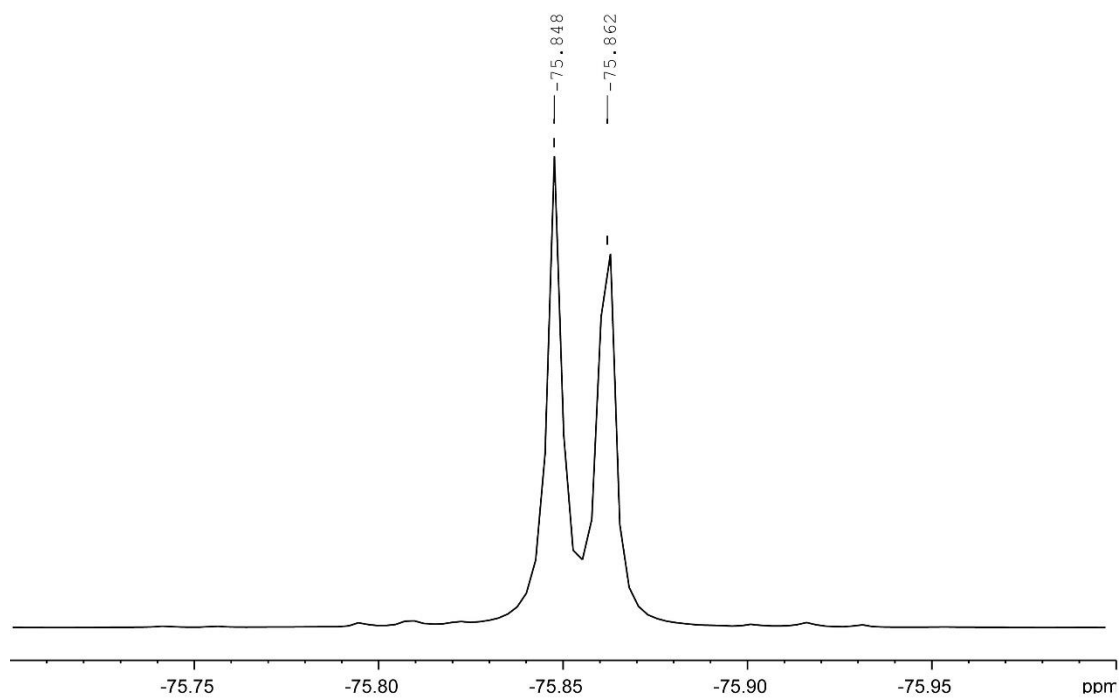


**Figure S22.**  $^{19}\text{F}$  NMR spectrum of halothane in  $\text{CDCl}_3$ .

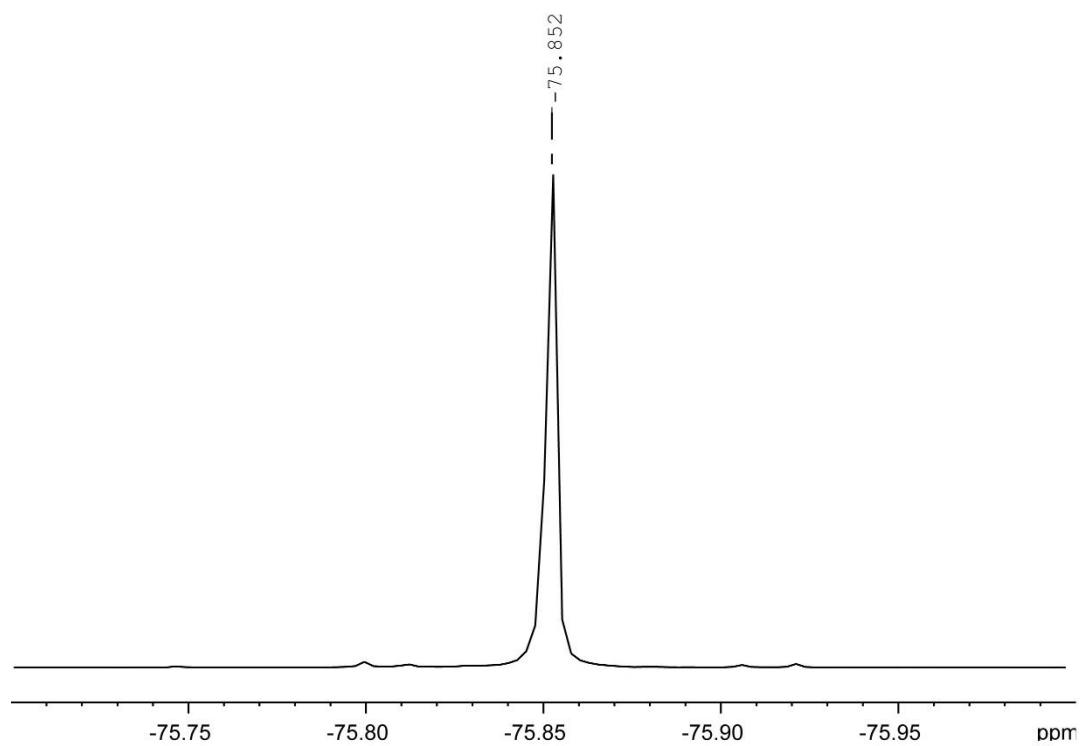


**Figure S23.**  $^{19}\text{F}$  (decouple from  $^1\text{H}$ ) NMR spectrum of halothane in  $\text{CDCl}_3$ .

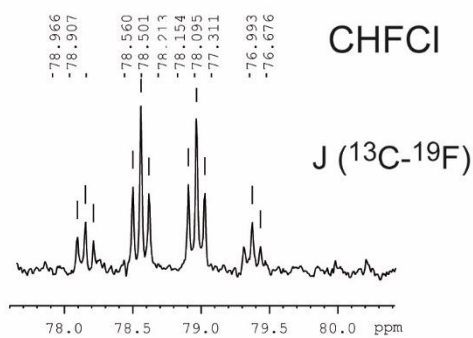
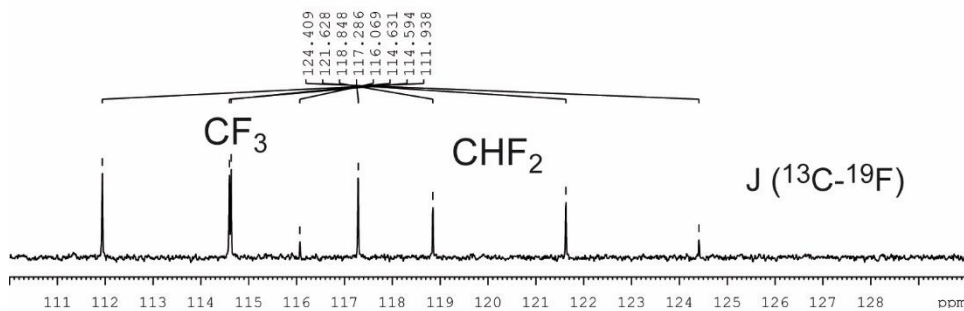
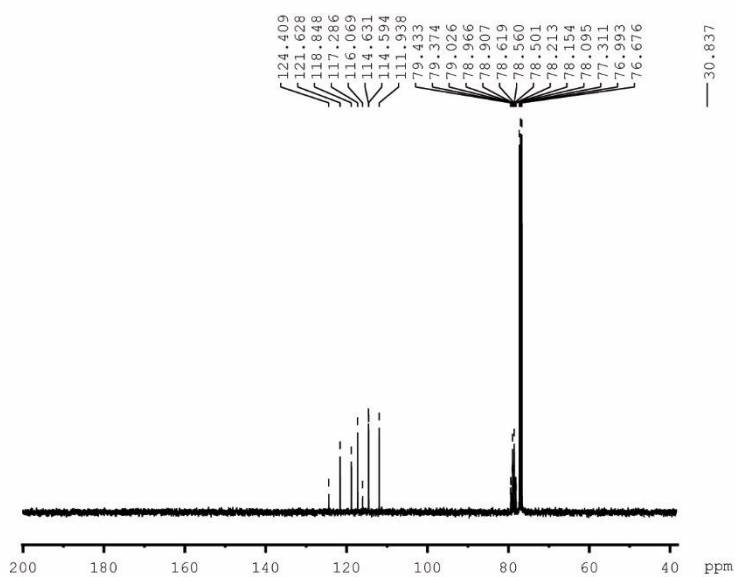


**Figure S24.** <sup>13</sup>C (decouple from <sup>1</sup>H) NMR spectrum of isoflurane in CDCl<sub>3</sub>.

## 9. $^1\text{H}$ , $^{19}\text{F}$ and $^{13}\text{C}$ Solid State NMR spectra

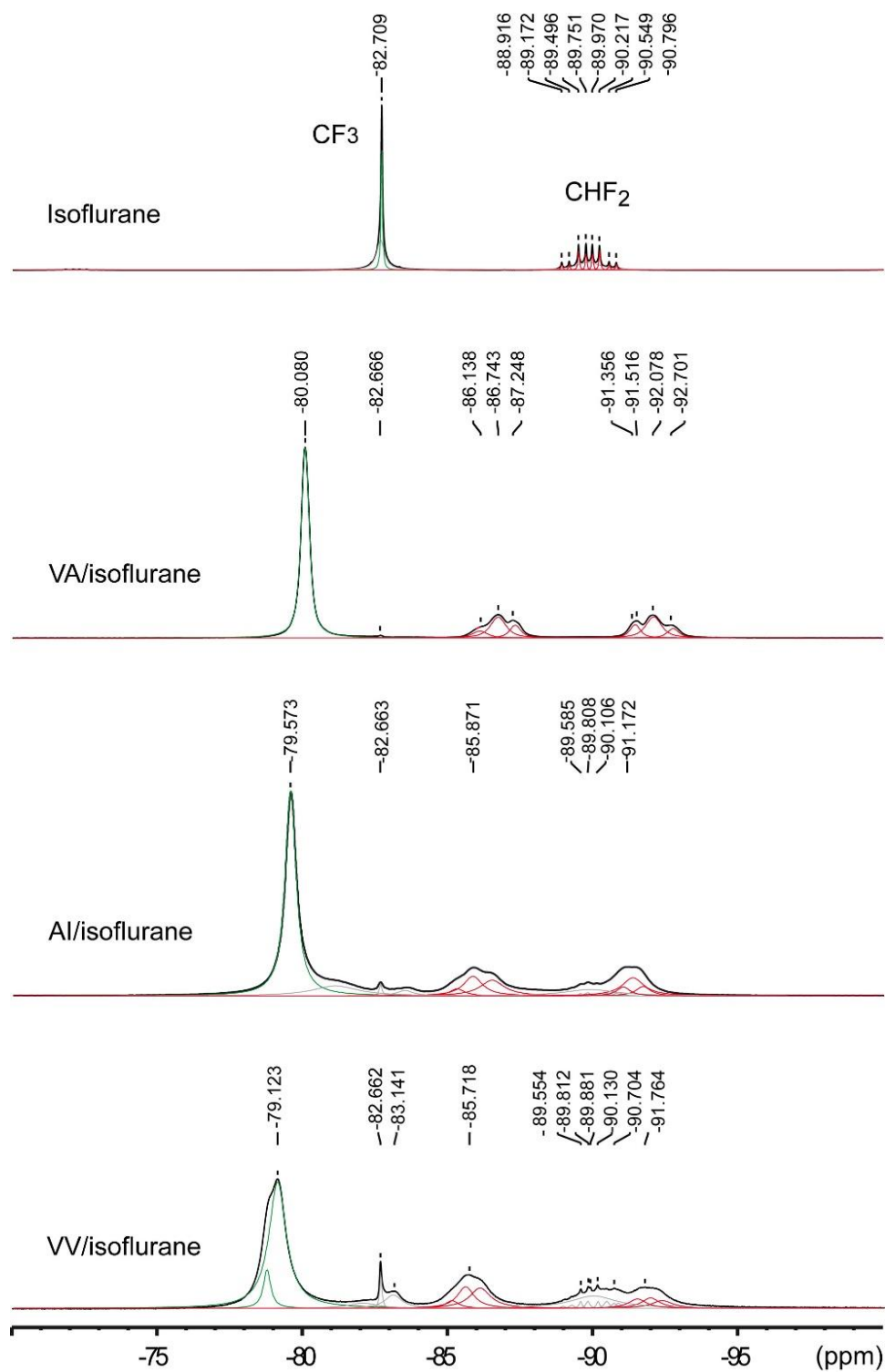


**Figure S25.**  $^{19}\text{F}$  SPE MAS NMR spectra of pure isoflurane (298K) and isoflurane in dipeptides (249K).

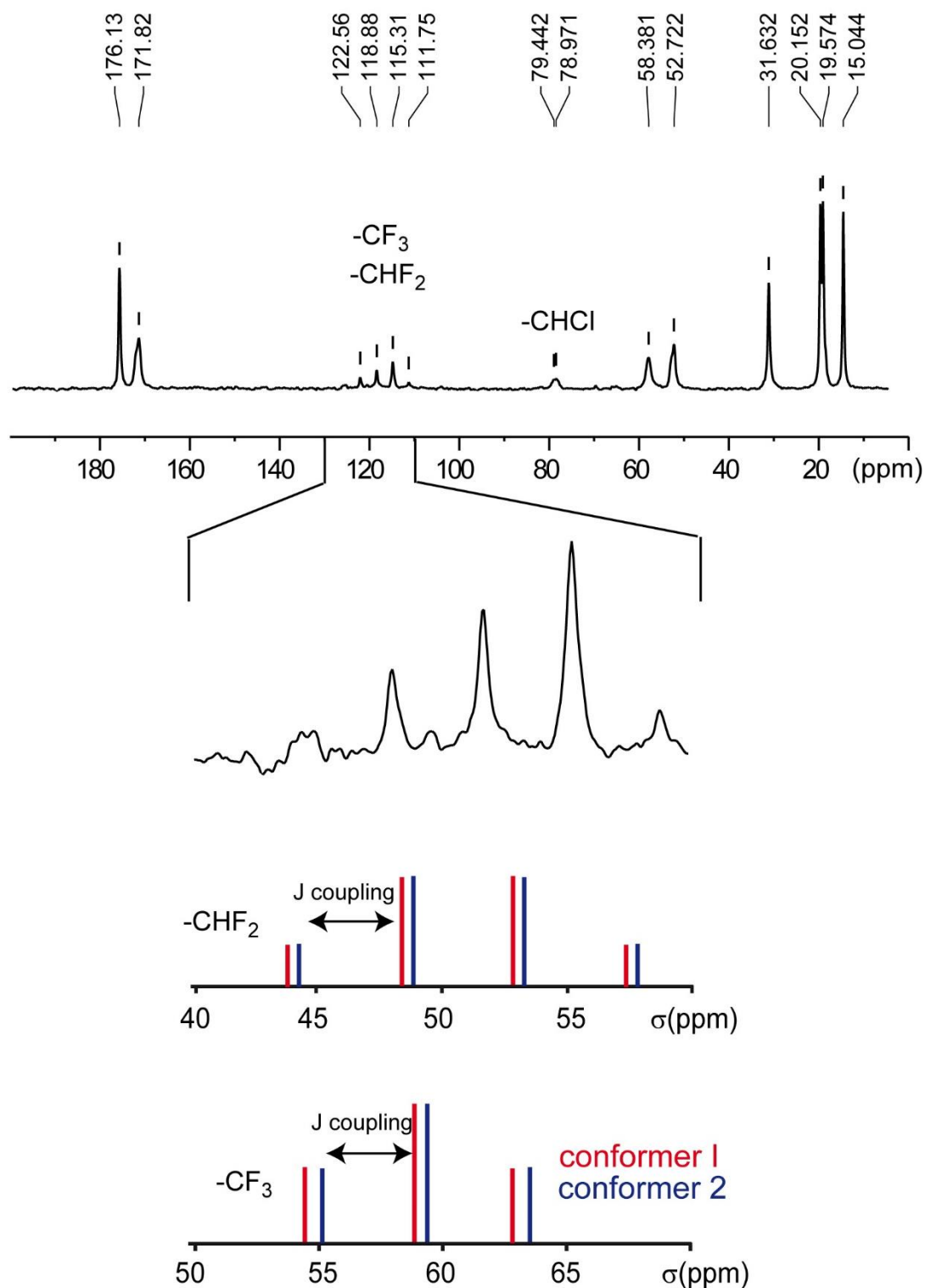


**Figure S26.**  $^{13}\text{C}\{^1\text{H}\}$  CP MAS NMR spectrum of isoflurane in VA at 249 K (ss= 8 kHz, ct= 5 ms) (above), predicted  $^{13}\text{C}$  chemical shifts of the two conformers (below).

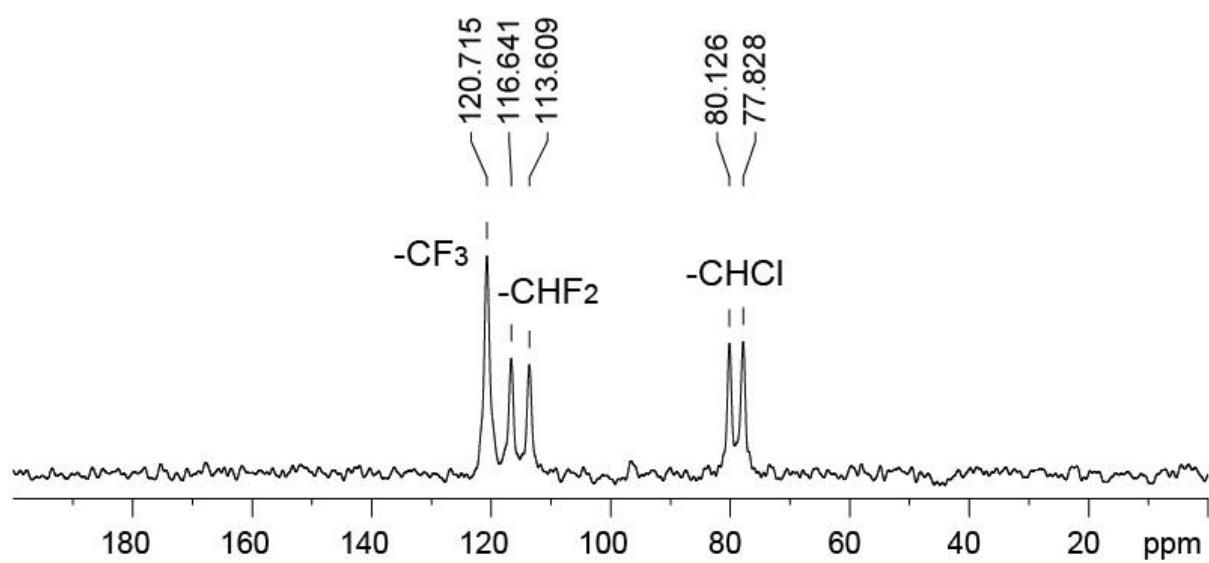


**Figure S27.**  $^{13}\text{C}\{^{19}\text{F}\}$  SPE MAS NMR spectrum of Isoflurane on celite. A spinning speed of 5 kHz was applied,  $\text{rd} = 30 \text{ s}$ ,  $T = 300 \text{ K}$ .

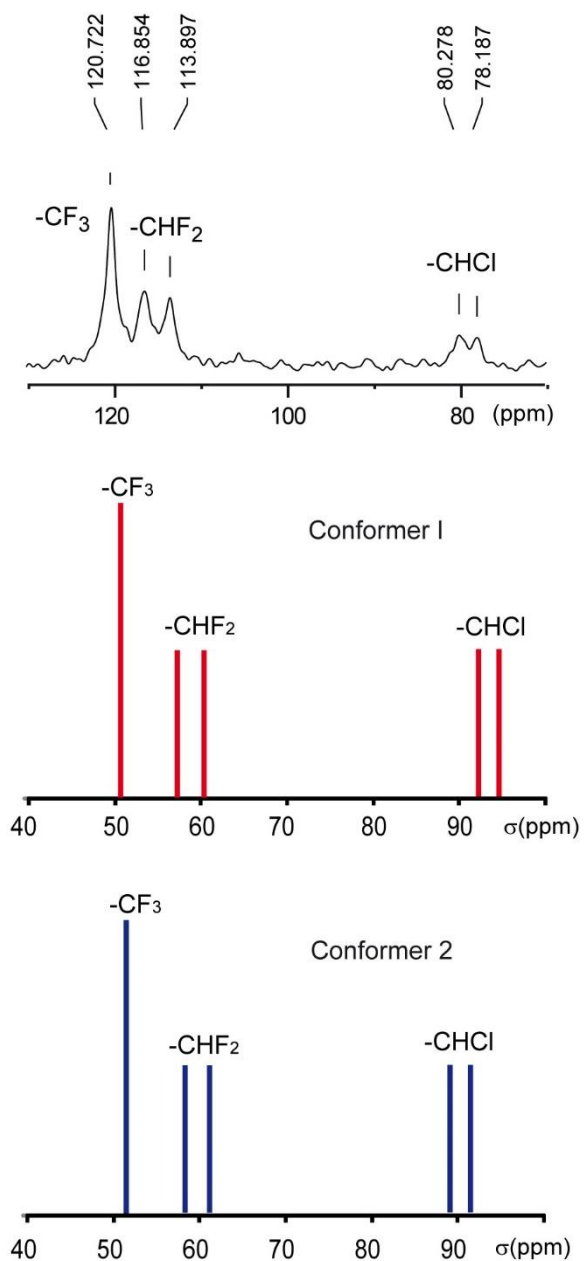


**Figure S28.**  $^{13}\text{C}\{^{19}\text{F}\}$  CP MAS NMR spectrum of isoflurane in VA at 249 K ( $ss = 8$  kHz,  $ct = 5$  ms) (above). Predicted  $^{13}\text{C}$  chemical shifts of the two conformers I and II (below).

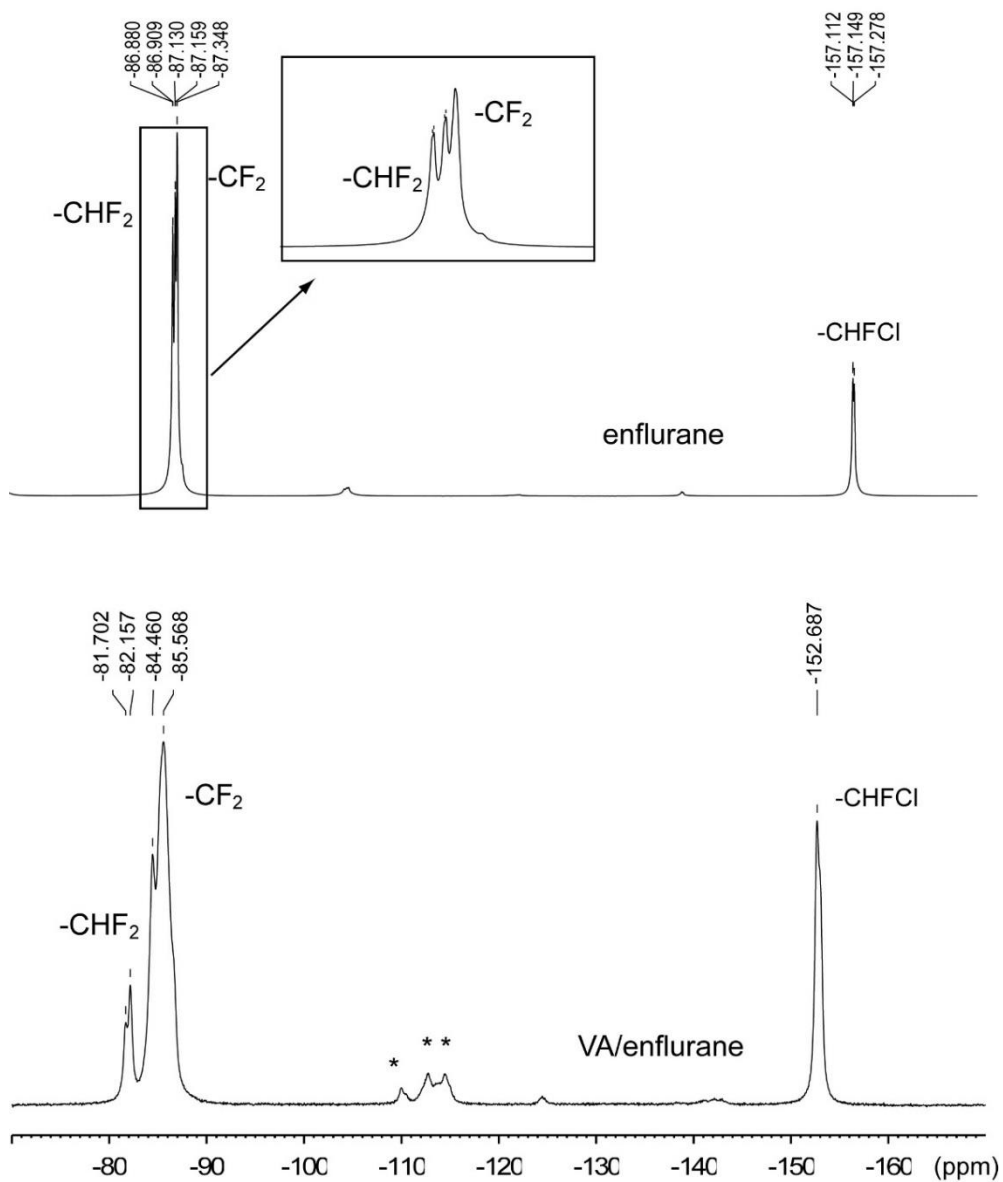


**Figure S29.**  $^{19}\text{F}$  SPE MAS NMR of enflurane on celite at 295K (ss= 5 kHz, rd= 20 s) (above) and VA/enflurane at 243K (ss= 8 kHz, rd= 20 s) (below).

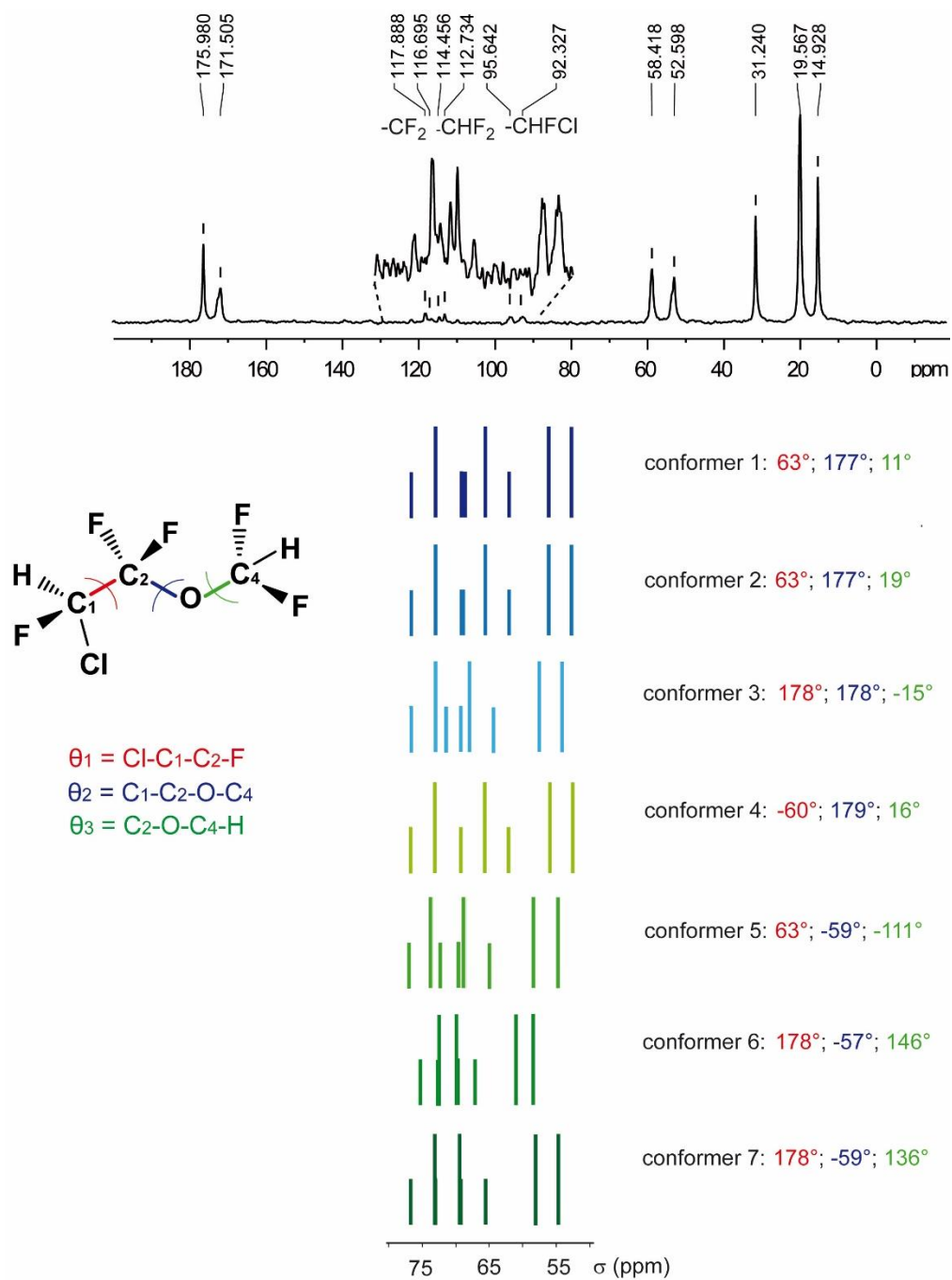


**Figure S30.**  $^{13}\text{C}\{^1\text{H}\}$  SPE MAS NMR spectrum of enflurane in VA at 300 K (ss= 12.5 kHz, rd=10s) (above). Calculated  $^{13}\text{C}$  shielding constants of the 7 conformers (below).

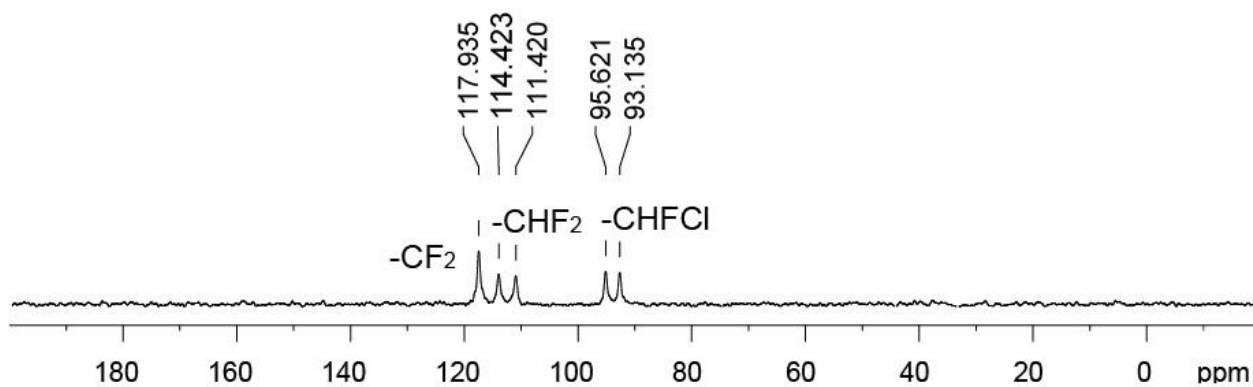


**Figure 31**  $^{13}\text{C}\{^{19}\text{F}\}$  MAS NMR spectrum of enflurane in celite,  $T = 300$  K.

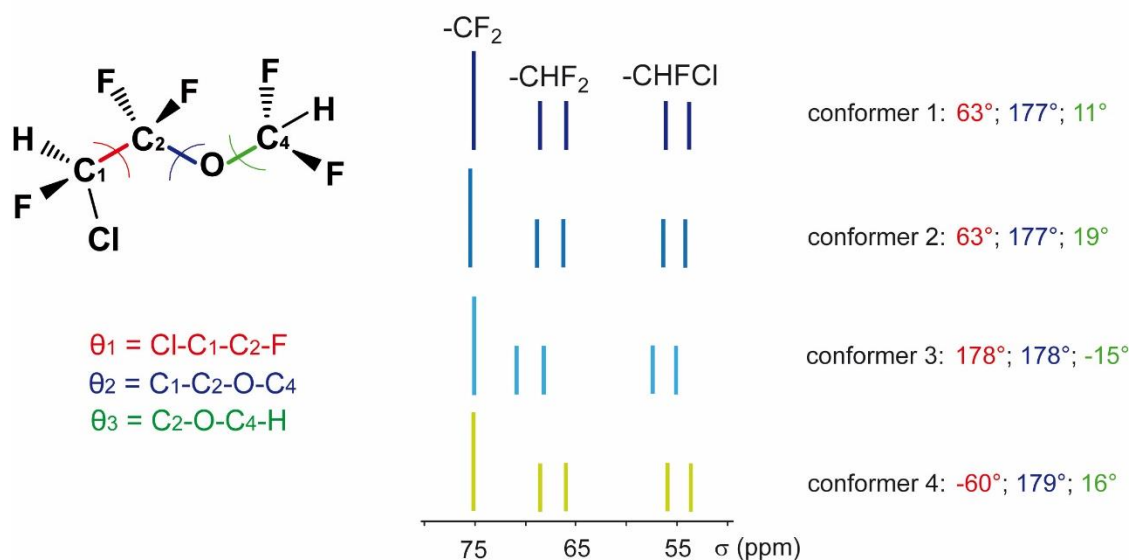
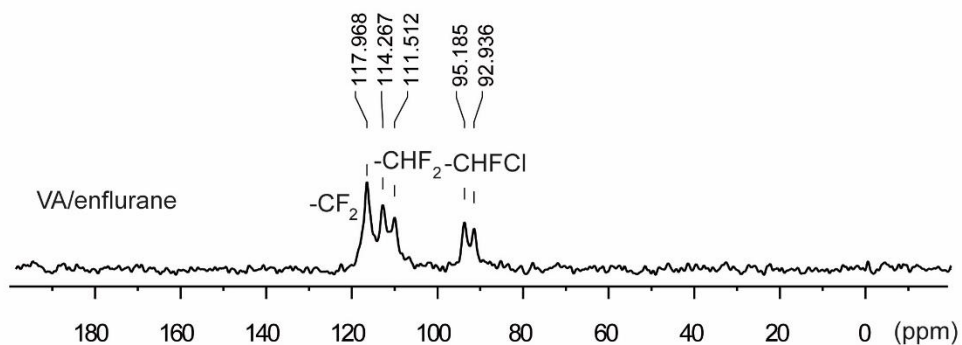


**Figure S32.**  $^{13}\text{C}\{^{19}\text{F}\}$  CPMAS NMR spectrum of enflurane in VA (above). A spinning speed of 8 kHz was applied,  $ct = 5$  ms,  $T = 243$  K. Calculated  $^{13}\text{C}$  shielding constants of the 4 conformers (below).

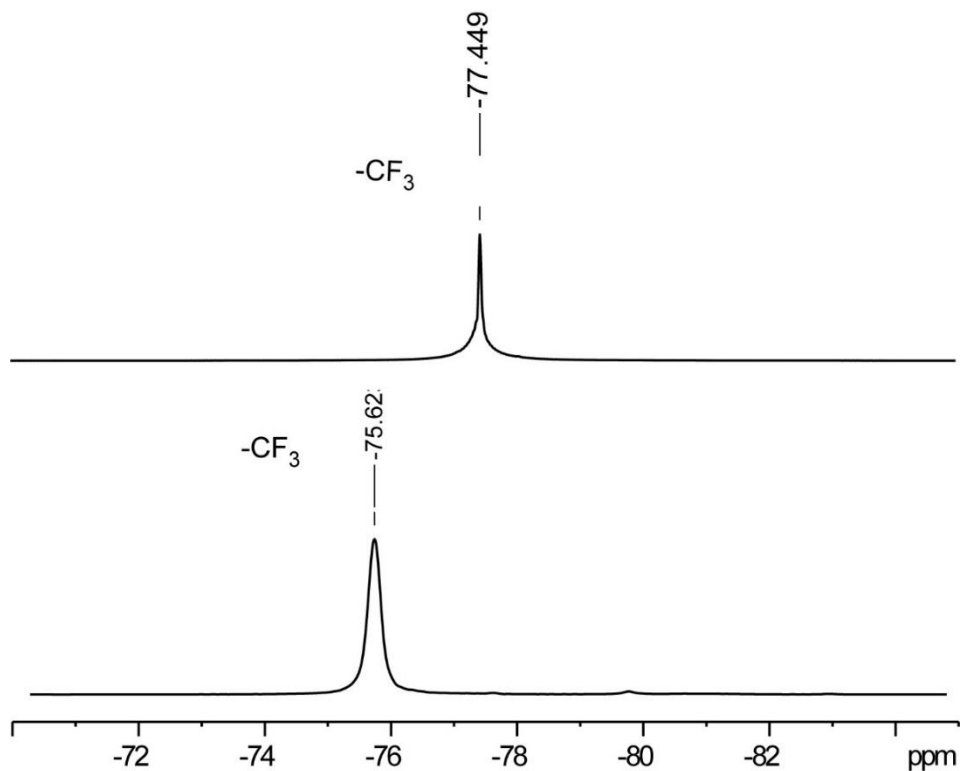


**Figure S33.**  $^{19}\text{F}$  SPE MAS NMR spectra of halothane on celite at 298K (above) and b) in VA at 269K (below).

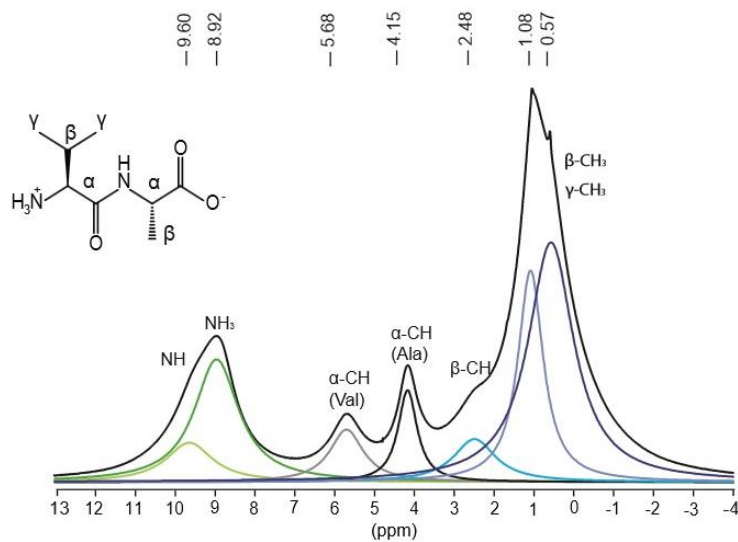


**Figure S34.**  $^1\text{H}$  SPE MAS NMR spectrum of L-Valyl-L-Alanine (VA) (600 MHz and 30 kHz spinning speed).

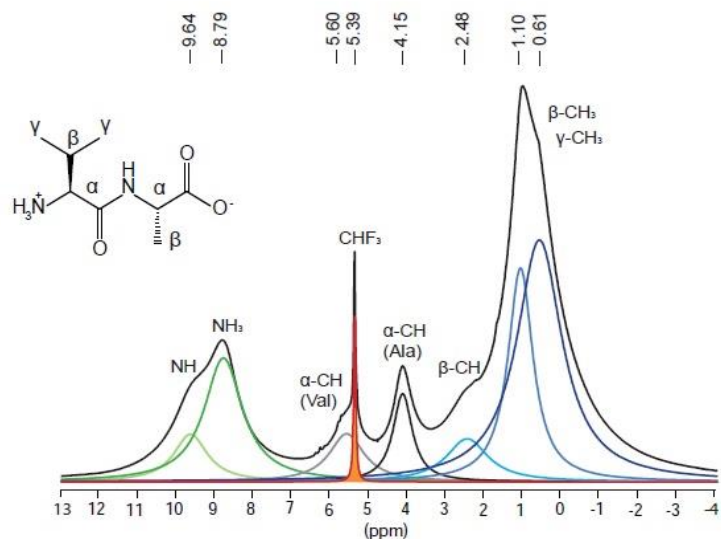


**Figure S35.** <sup>1</sup>H SPE fast-MAS NMR spectrum of VA/Halothane (600 MHz and 30 kHz spinning speed).

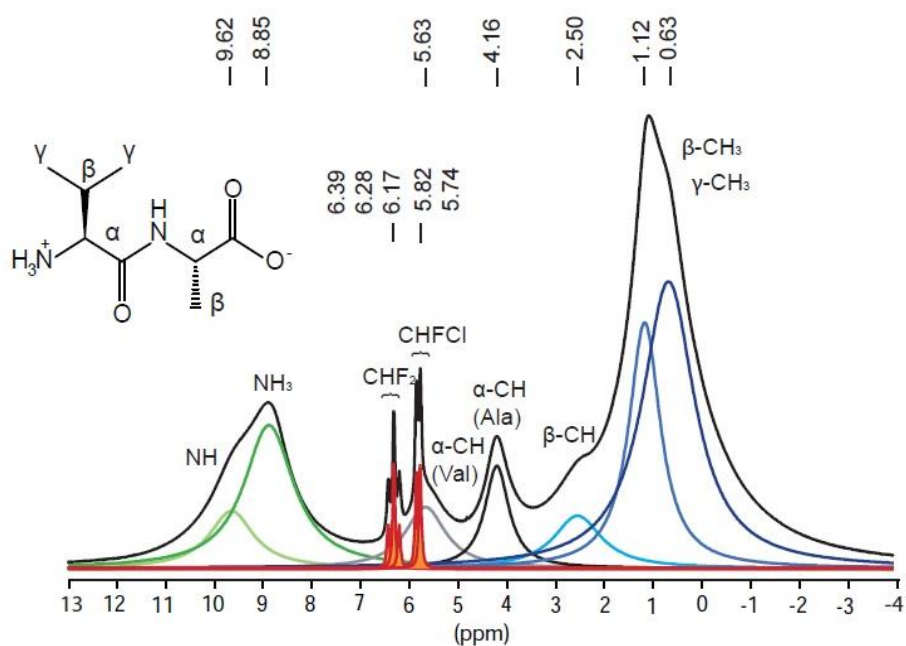


**Figure S36.** <sup>1</sup>H SPE fast-MAS NMR spectrum of VA/Enflurane (600 MHz and 30 kHz spinning speed).

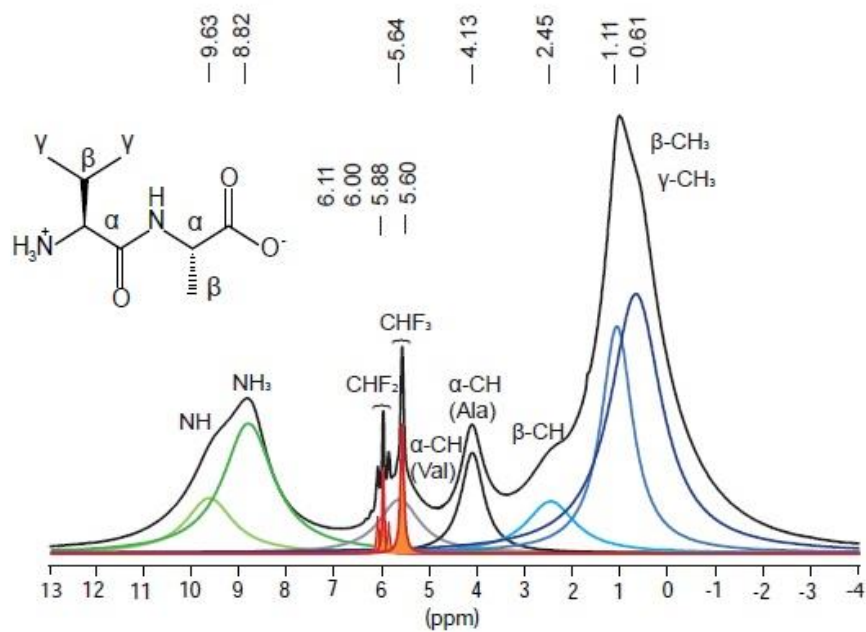


**Figure S37.**  $^1\text{H}$  SPE fast-MAS NMR spectrum of VA/Isoflurane (600 MHz and 30 kHz spinning speed).

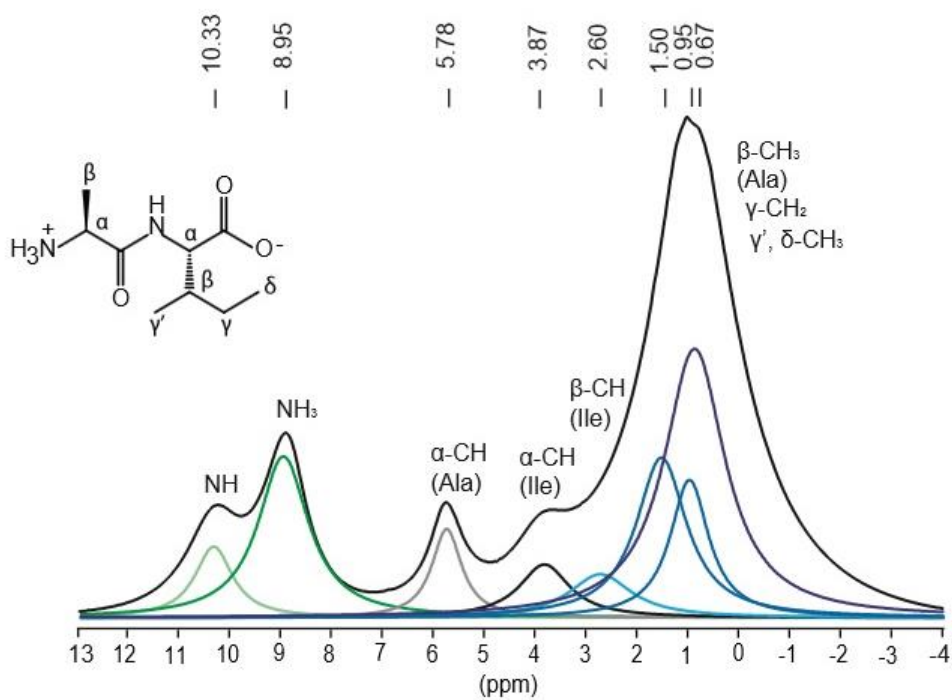


**Figure S38.**  $^1\text{H}$  SPE fast-MAS NMR spectrum of L-Alanyl-L-Isoleucine (AI) (600 MHz and 30 kHz spinning speed).

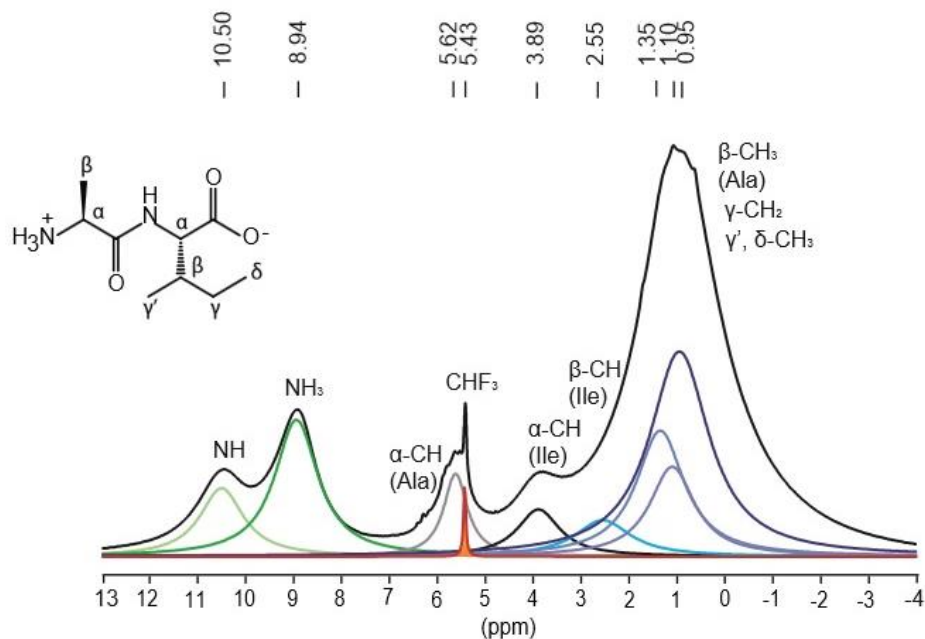


**Figure S39.** <sup>1</sup>H SPE fast-MAS NMR spectrum of Al/Halothane (600 MHz and 30 kHz spinning speed).

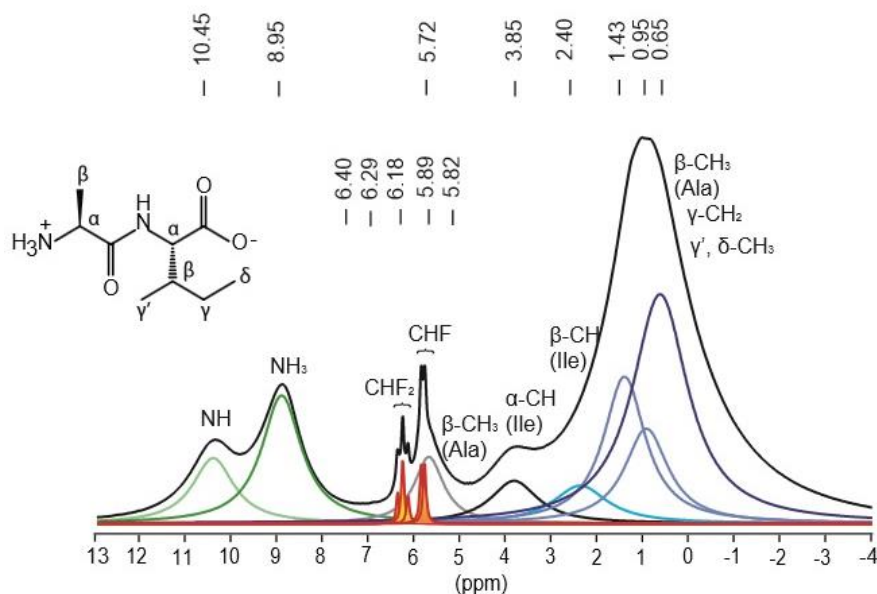


**Figure S40.** <sup>1</sup>H SPE fast-MAS NMR spectrum of Al/Enflurane (600 MHz and 30 kHz spinning speed).

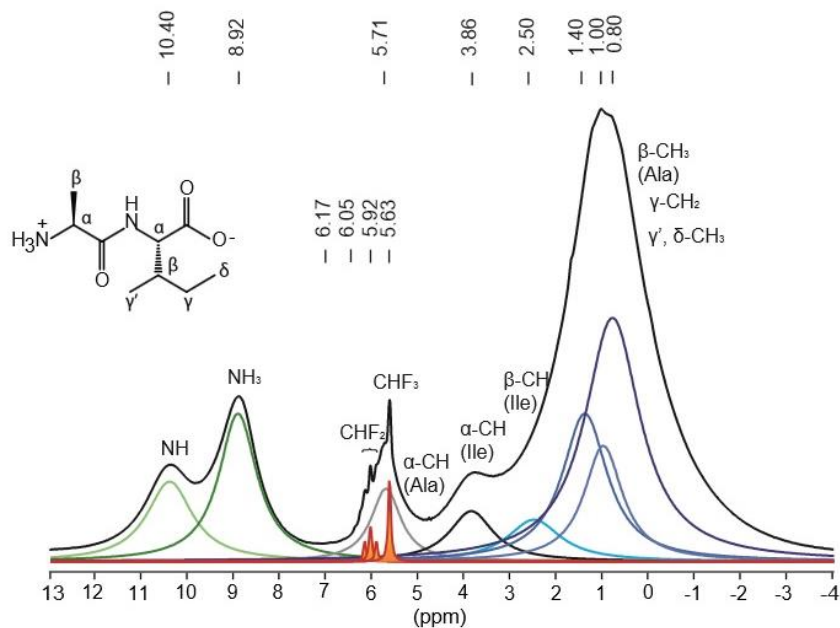


**Figure S41.** <sup>1</sup>H SPE fast-MAS NMR spectrum of Al/Isoflurane (600 MHz and 30 kHz spinning speed).

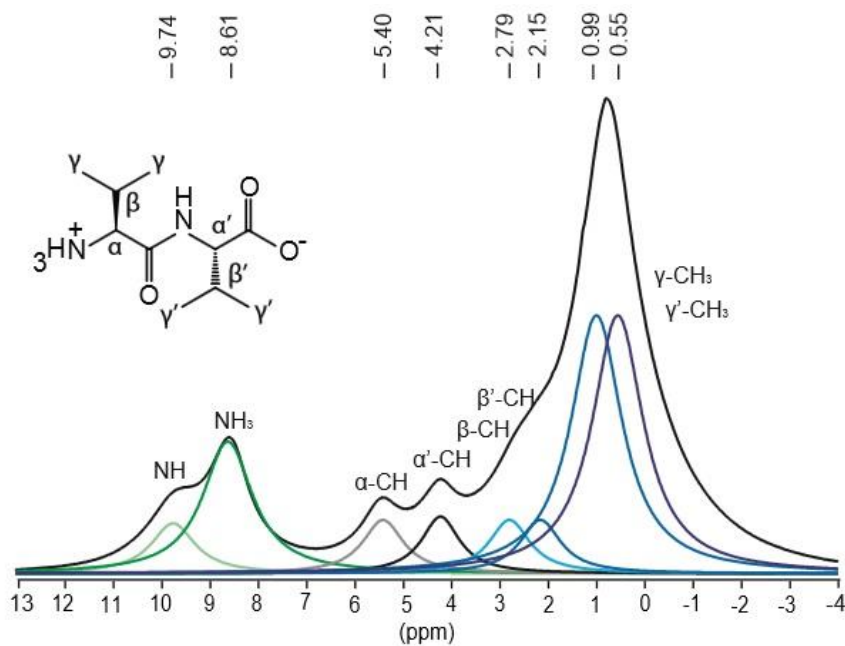


**Figure S42.** <sup>1</sup>H SPE fast-MAS NMR spectrum of L-Valyl-L-Valine (VV) (600 MHz and 30 kHz spinning speed).

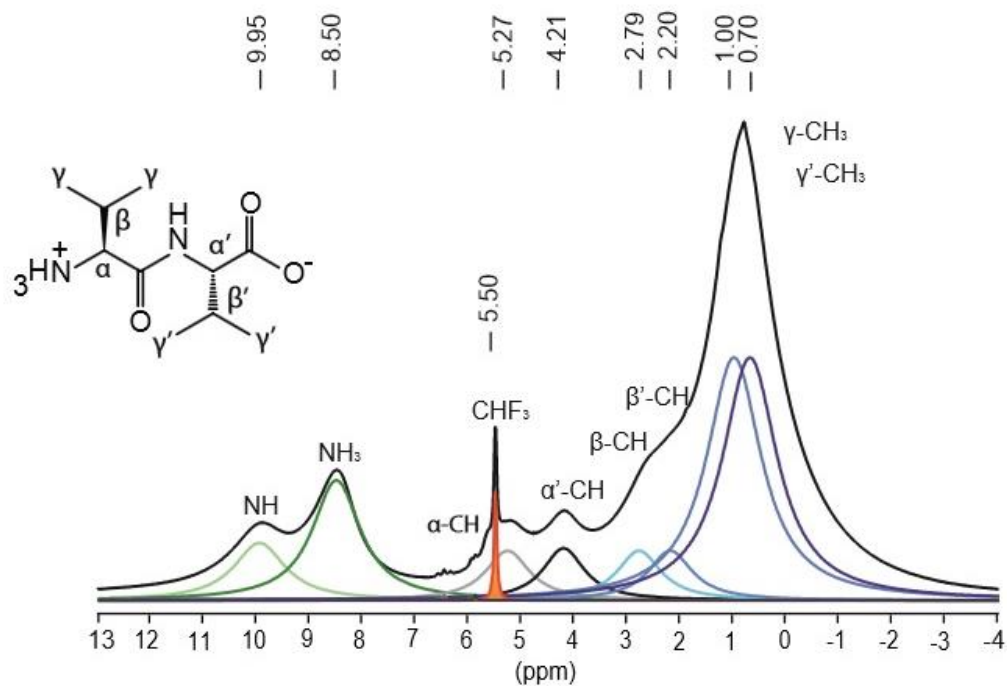


**Figure S43.** <sup>1</sup>H SPE fast-MAS NMR spectrum of VV/Halothane (600 MHz and 30 kHz spinning speed).

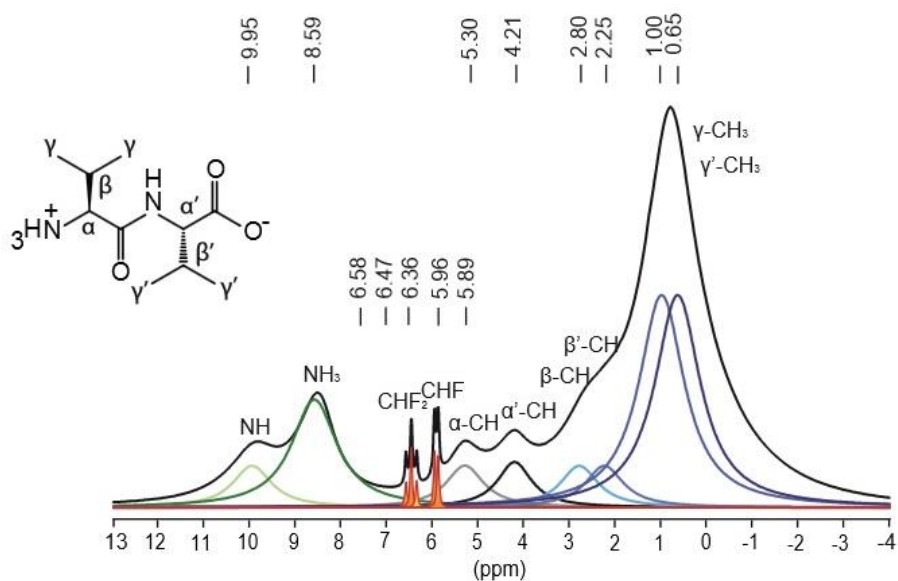


**Figure S44.** <sup>1</sup>H SPE fast-MAS NMR spectrum of VV/Enflurane (600 MHz and 30 kHz spinning speed).

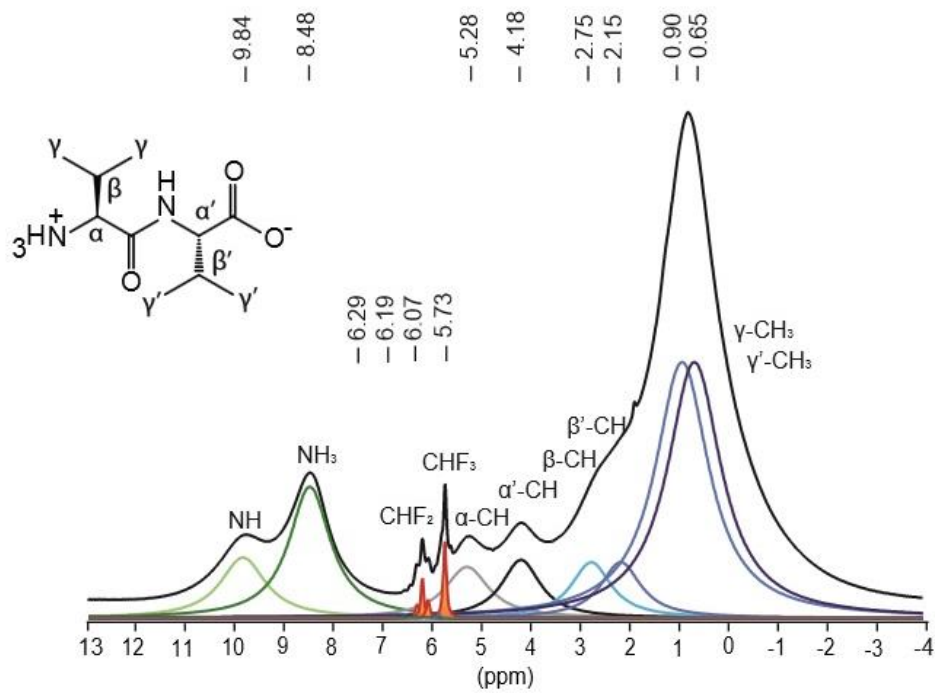


**Figure S45.** <sup>1</sup>H SPE fast-MAS NMR spectrum of VV/Isoflurane (600 MHz and 30 kHz spinning speed).

## 10. Kinetics of adsorption experiments

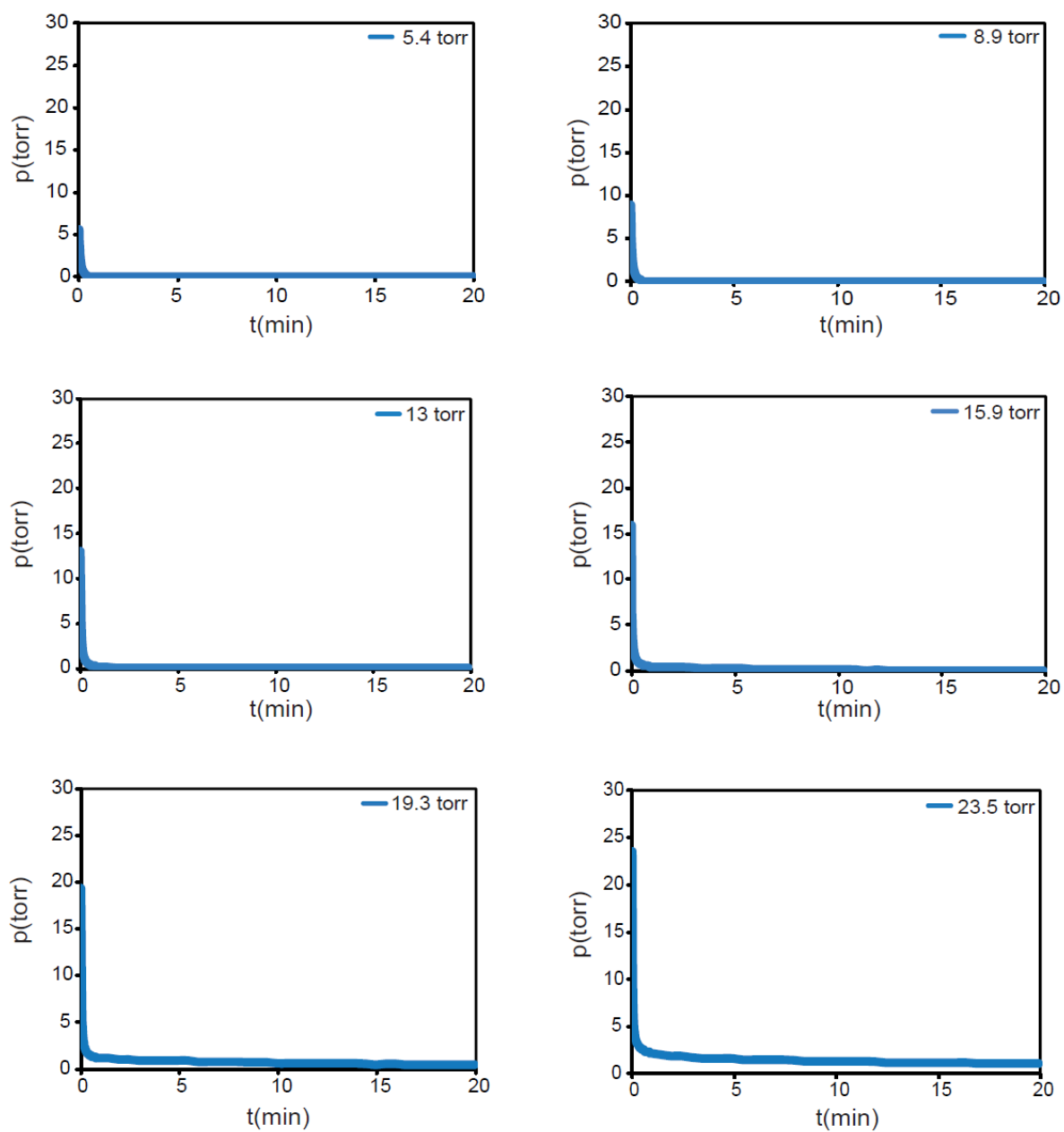


**Figure S46.** Kinetics of adsorption of enflurane in VA at 273 K.

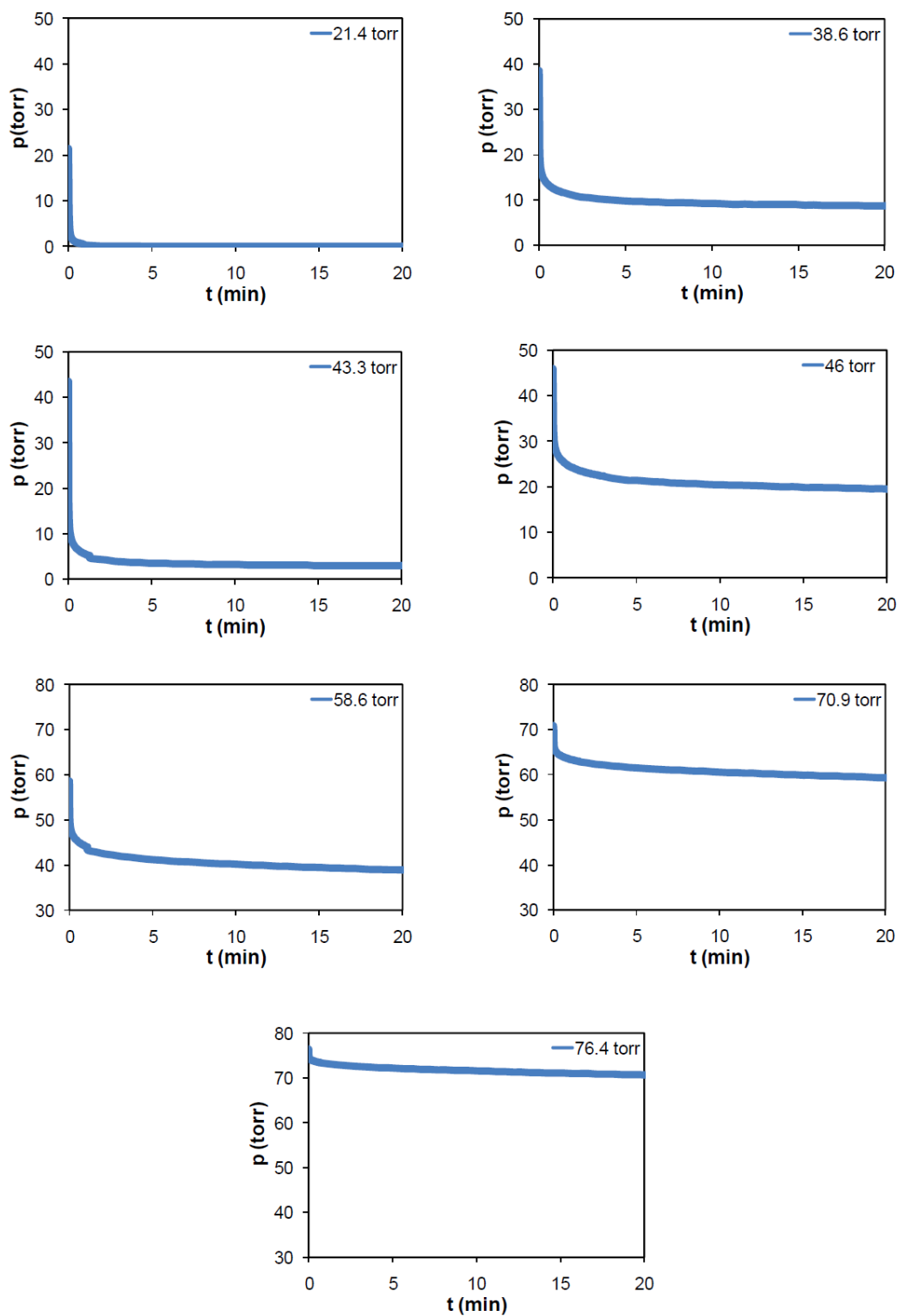


**Figure S47.** Kinetics of adsorption of isoflurane in VA at 273 K.

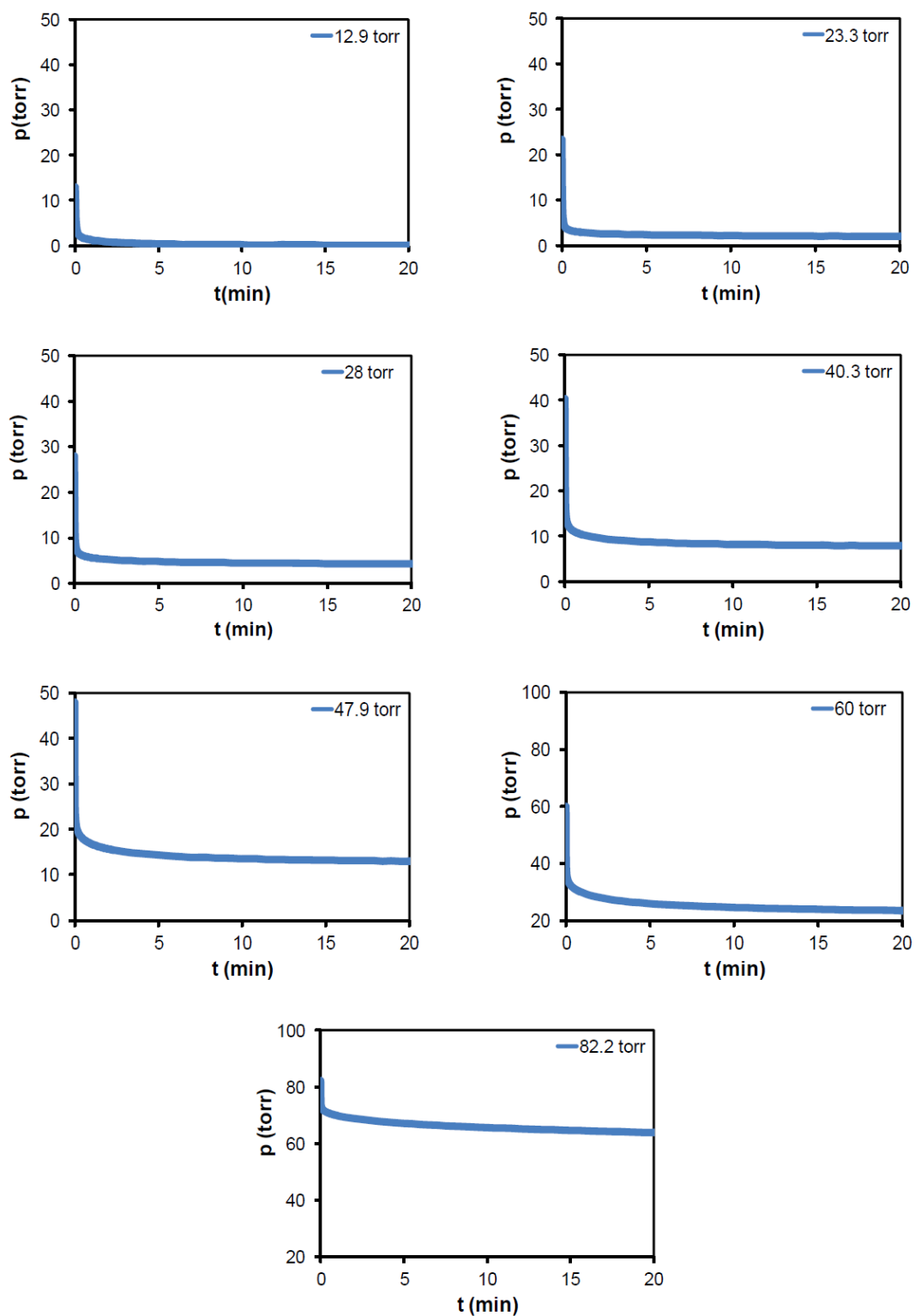


**Figure S48.** Kinetics of adsorption of halothane in VA at 273 K.

## 11. Adsorption and desorption curves

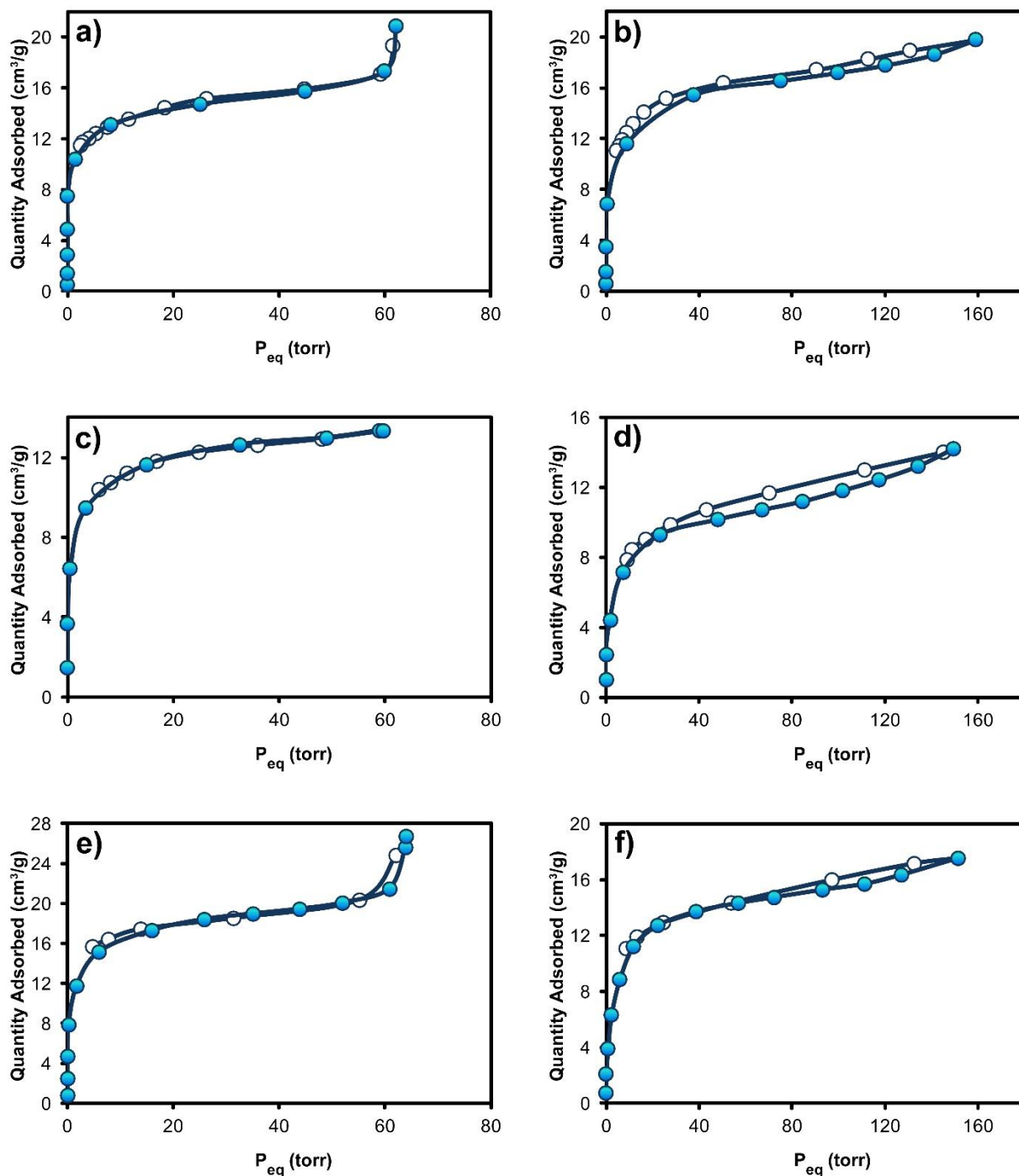


**Figure S49.** Adsorption/desorption isotherms of enflurane in VA at 273K (a) and 298K (b), in AI at 273K (c) and 298K (d), and in VV at 273K (e) and 298K (f).

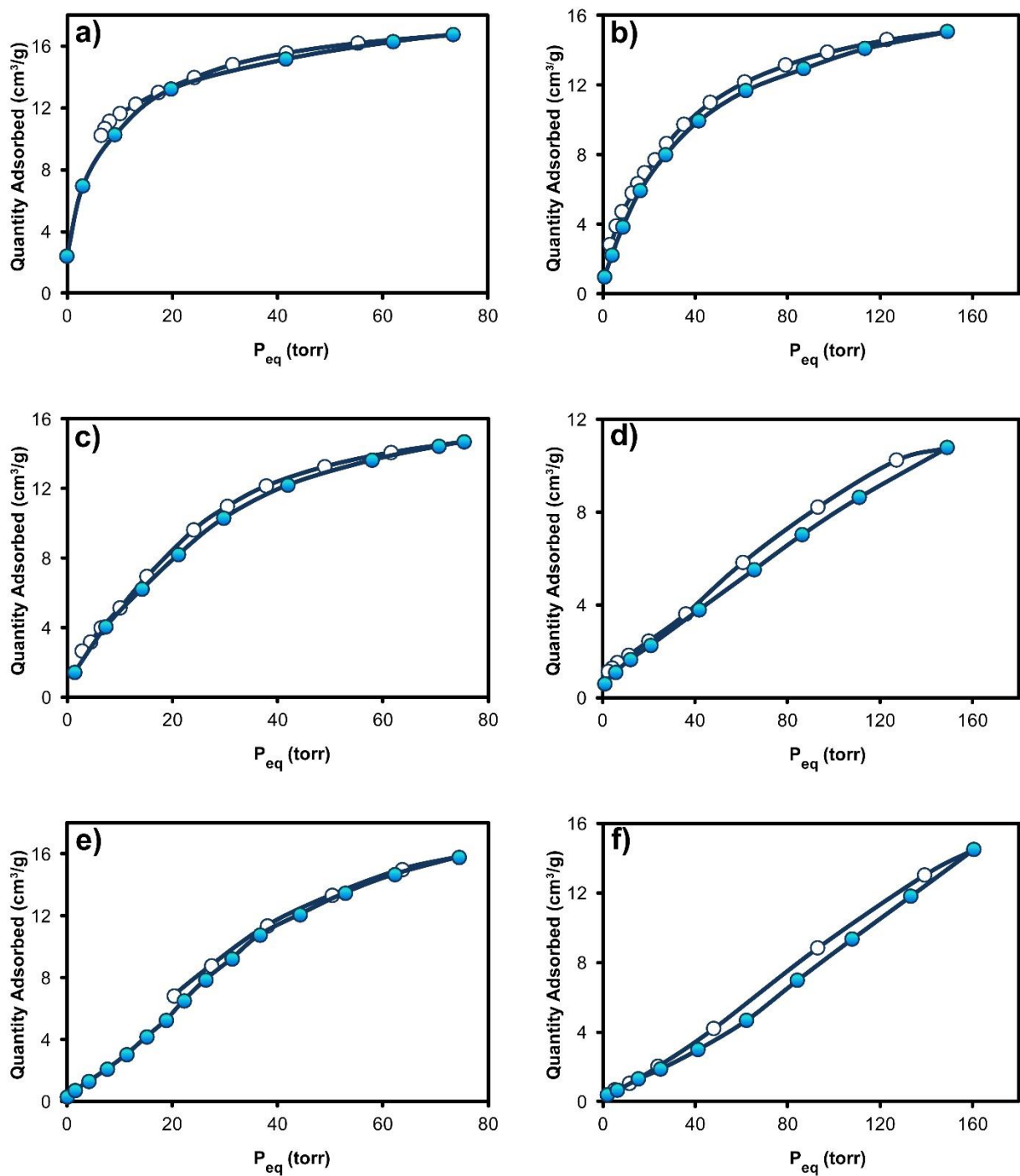


**Figure S50.** Adsorption/desorption isotherms of isoflurane in VA at 273K (a) and 298K (b), in AI at 273K (c) and 298K (d), and in VV at 273K (e) and 298K (f).

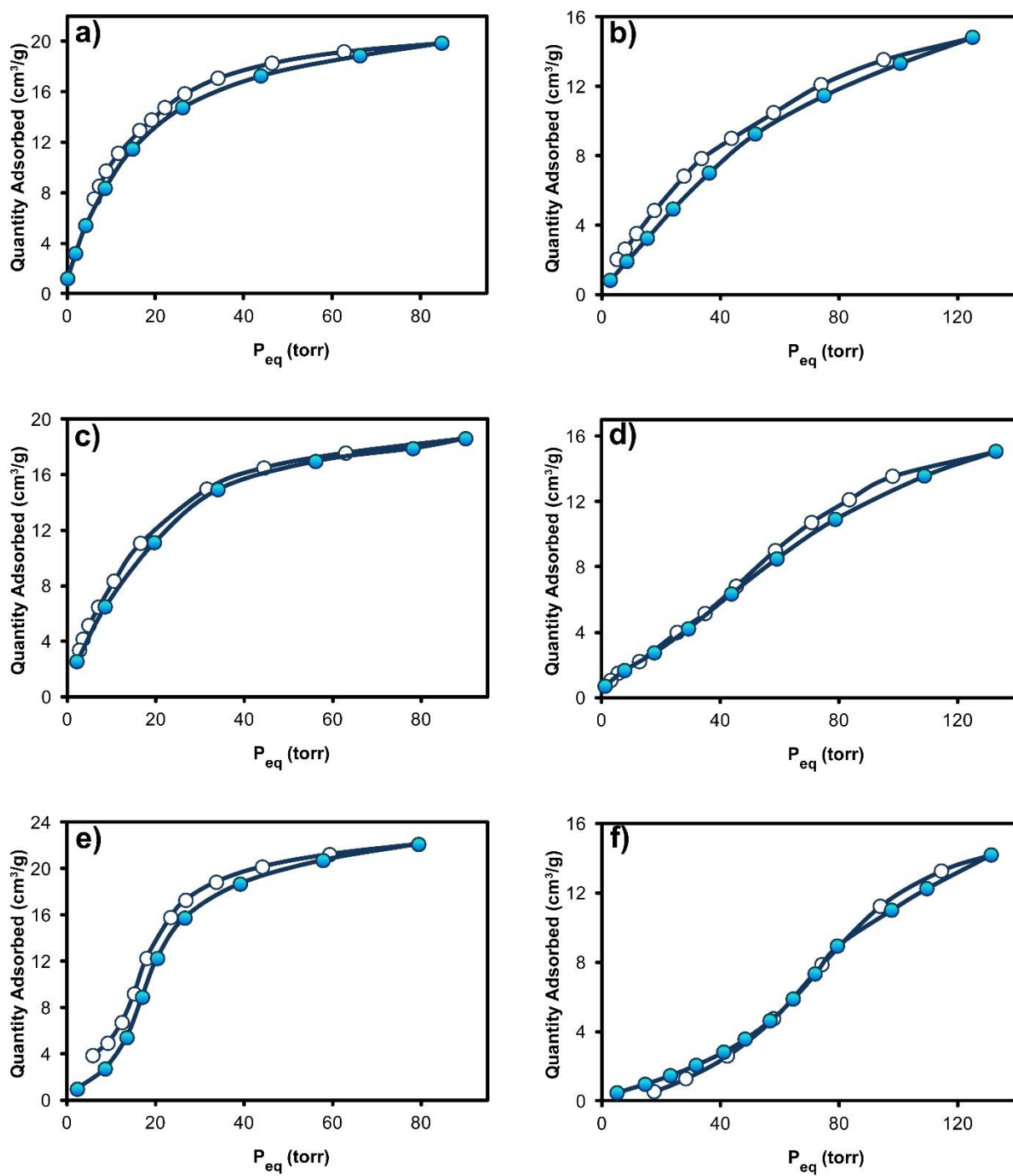


**Figure S51.** Adsorption/desorption isotherms of alothane in VA at 273K (a) and 298K (b), in AI at 273K (c) and 298K (d), and in VV at 273K (e) and 298K (f).

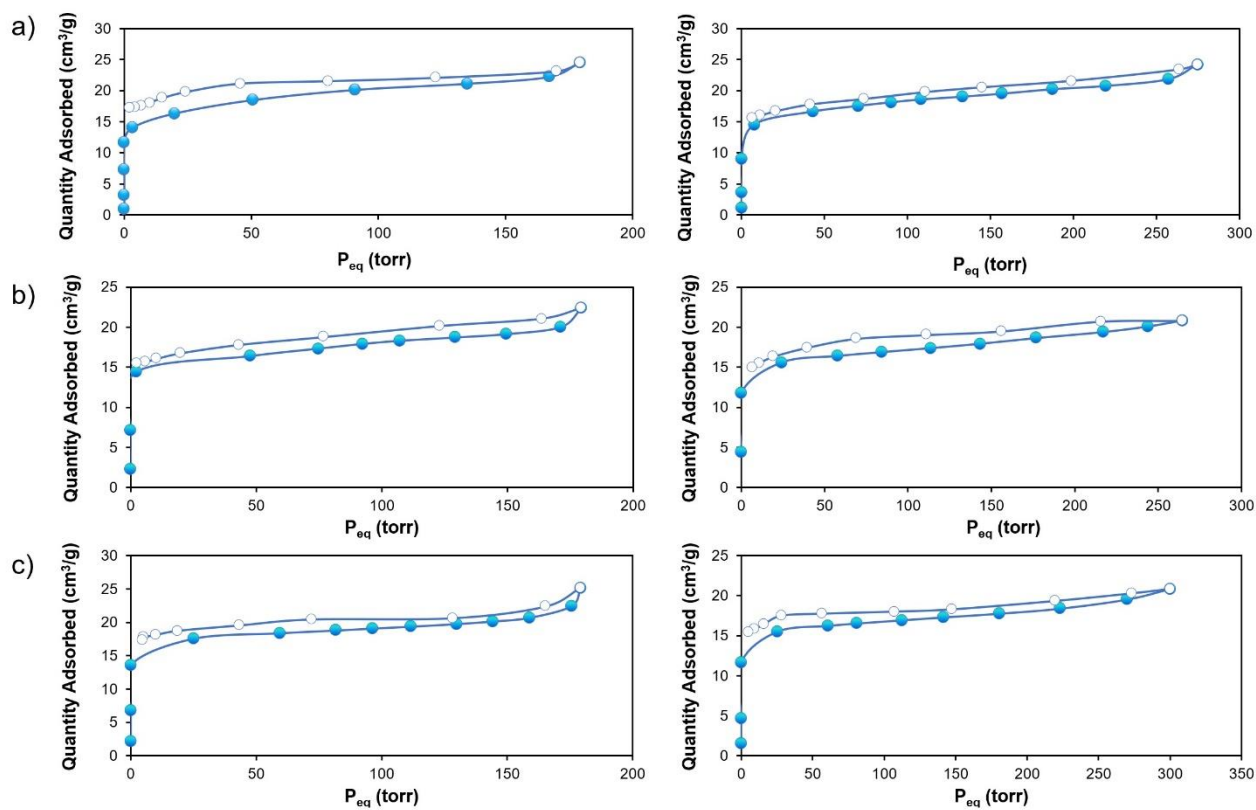


**Figure S52.** Adsorption (full circles) and desorption (empty circles) isotherms at 273 (left) and 298 K (right) of diethyl ether: (a) in VA, (b) in AI and (c) in VV.

## 12. GCMC simulation of isotherms

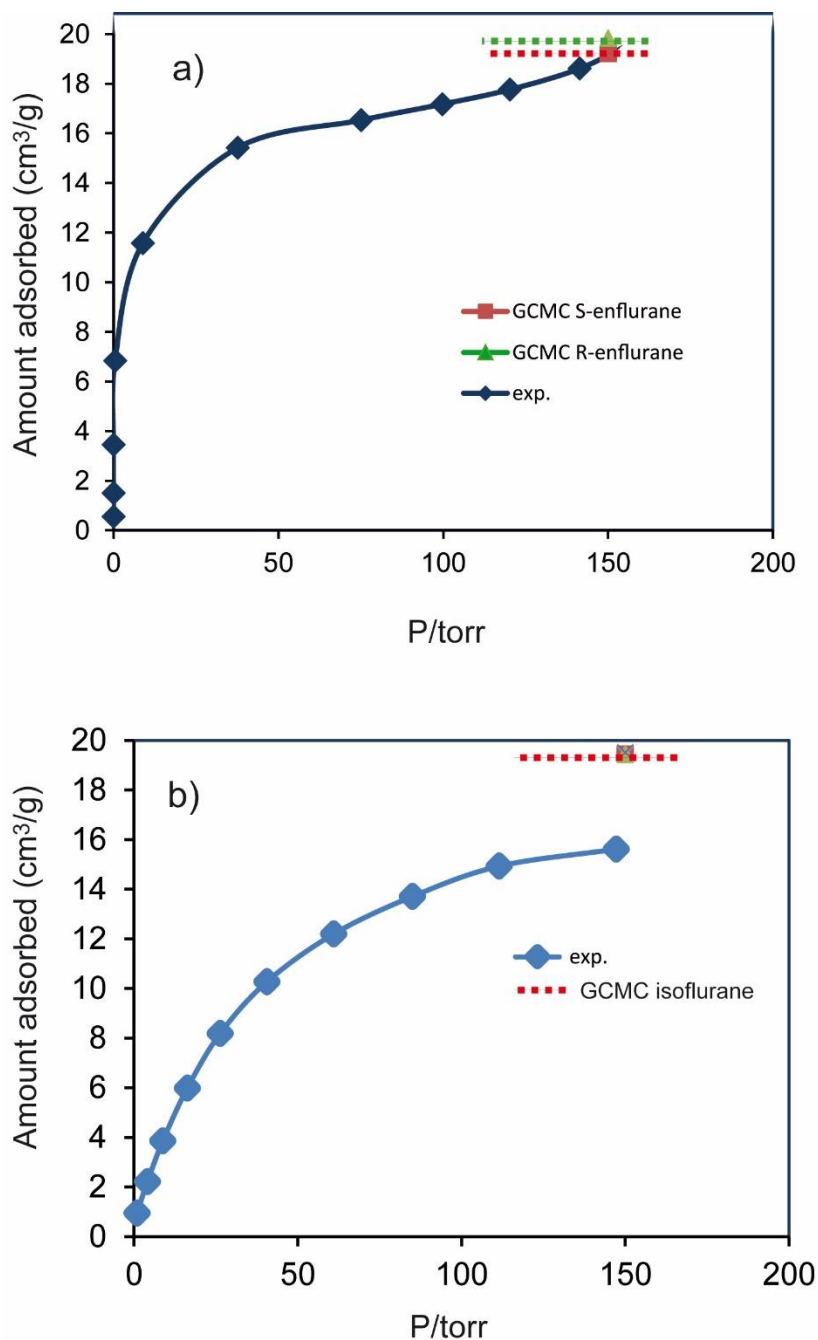


**Figure S53.** Enflurane (a) and isoflurane (b) adsorption isotherms in VA. The experimental isotherms are compared to the maximum adsorption values calculated by GCMC simulation. Adsorption values of R- and S- enflurane are 19.2 and 19.8 cm<sup>3</sup>/g, respectively. Adsorption values of isoflurane for conformers I and II and in both configurations correspond to 19.51 cm<sup>3</sup>/g.

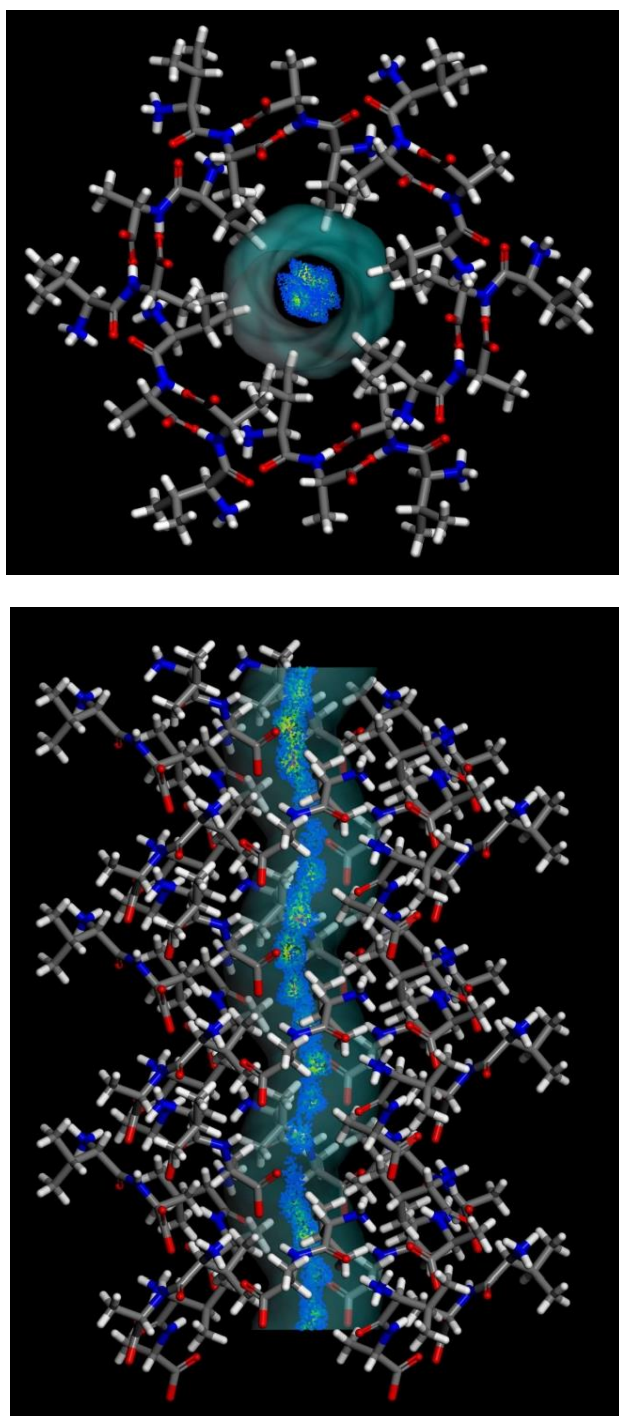


**Figure S54.** Crystal structure of VA, as viewed along the channel axis (above) and perpendicular to the channel axis (below), showing the mass centers of enflurane as determined by the GCMC simulation of enflurane adsorption at 298K and at a pressure of 150 torr. The conformation of enflurane corresponds to the conformer of minimum energy as determined by ab initio calculations ( $\theta_1= 63^\circ$ ,  $\theta_2= 177^\circ$  and  $\theta_3= 11^\circ$ ). Adsorption values of the two enantiomers of enflurane are 19.2 and 19.8  $\text{cm}^3/\text{g}$ , in agreement with the experimental value of 19.8  $\text{cm}^3/\text{g}$ .

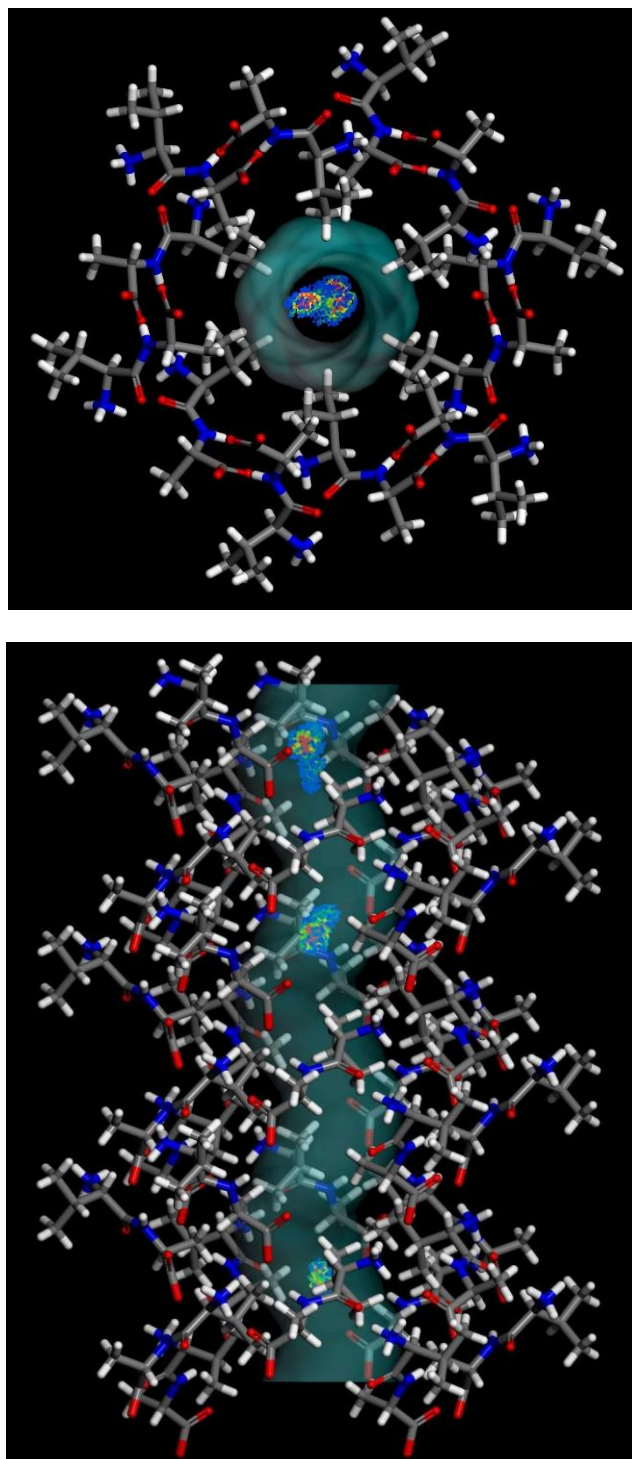


**Figure S55.** Crystal structure of VA, as viewed along the channel axis (above) and perpendicular to the channel axis (below), showing the mass centers of S-isoflurane as determined by the GCMC simulation of isoflurane adsorption at 298K and at a pressure of 150 torr. The conformation of isoflurane corresponds to the conformer II as determined by ab initio calculations.

### 13. Dynamic Light Scattering

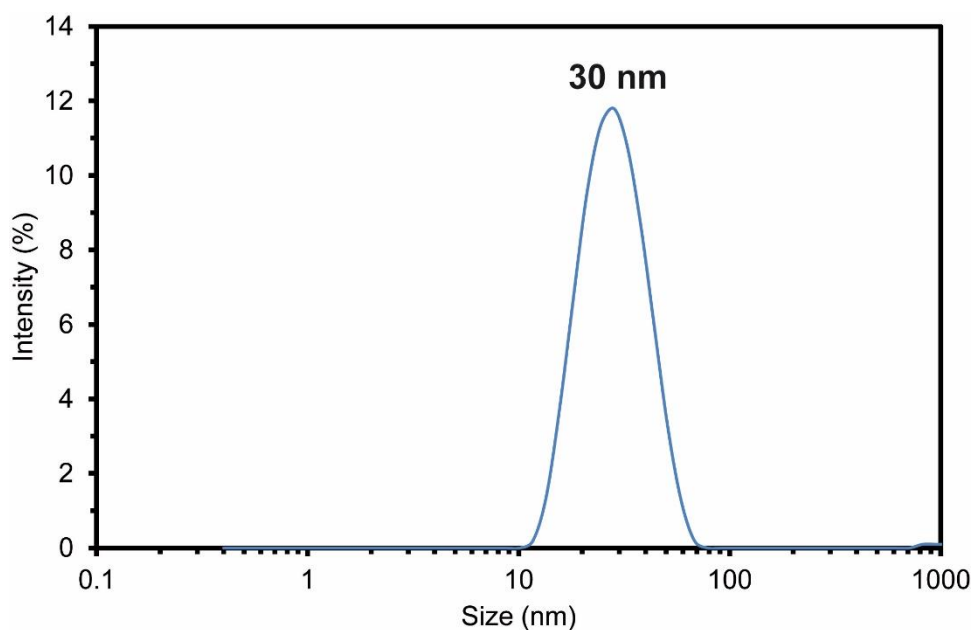


**Figure S56.** Particle size distribution of the VA crystals. The distribution size is centered at 30 nm.

### 14. References

1. C. H. Gorbitz, E. Gundensen, *Acta Crystallogr., Sect. C: Cryst. Struct. Commun.* 1996, 52, 1764.
2. I. Moudrakosvski, D. V. Soldatov, J. A. Ripmeester, D. N. Sears, C. J. Jameson, *Proc. Natl. Acad. Sci. USA* 2004, 101, 17924.
3. C. H. Gorbitz, *New J. Chem.* 2003, 27, 1789.
4. A. Comotti, A. Fraccarollo, S. Bracco, M. Beretta, G. Distefano, M. Cossi, L. Marchese, C. Riccardi, P. Sozzani, *Cryst. Eng. Comm.*, 2013, 15, 1503.